



VCU

Virginia Commonwealth University
VCU Scholars Compass

Theses and Dissertations

Graduate School

2021

Sickle cell disease associated lipid changes and their relevance towards the disease pathogenesis And Lipid Biomarkers and Embryo Quality in In Vitro Fertilization; Pregnancy Success Differentially Expressed by Body Weight

Suad Alshammari

Follow this and additional works at: <https://scholarscompass.vcu.edu/etd>

© The Author

Downloaded from

<https://scholarscompass.vcu.edu/etd/6851>

This Thesis is brought to you for free and open access by the Graduate School at VCU Scholars Compass. It has been accepted for inclusion in Theses and Dissertations by an authorized administrator of VCU Scholars Compass. For more information, please contact libcompass@vcu.edu.

**Sickle cell disease associated lipid changes and their relevance towards the
disease pathogenesis**

And

**Lipid Biomarkers and Embryo Quality in In Vitro Fertilization; Pregnancy Success
Differentially Expressed by Body Weight**

**A thesis submitted in partial fulfillment of the requirements for the
degree of Master of Science at Virginia Commonwealth University.**

By

Suad Alshammari

Director:

Dayanjan S Wijesinghe

Virginia Commonwealth University

Richmond, Virginia

12, 2021

Acknowledgment

I would like to express my special thanks to my principal supervisor Dr. Dayanjan S Wijesinghe who guided me through my education and gave me the opportunities to achieve these projects. Also, I would thank my colleagues for their help and supports. A special thanks to my family for their supports through my journey.

TABLE OF CONTENTS

Contents

Table of Figures:.....	5
Chapter 1:.....	6
Sickle cell disease associated lipid changes and their relevance towards the disease pathogenesis: Literature Review	6
Introduction.....	8
1 Background	8
2 Pathophysiology	9
3 SCD Genotypes differentiation.....	10
4 Global burden of SCD:	15
5 SCD cell Disease in Saudi Arabia and the U.S	16
6 Clinical manifestation and complication of SCD	17
7 Method:.....	18
8 Clinical manifestation and changes on lipidome in SCD.....	22
8.1 Pain and VOC.....	22
8.2 Acute chest syndrome (ACS)	25
8.3 Hyper-coagulopathy and SCD	26
9 Treatments	29
9.1 Hydroxyurea	29
9.2 L-glutamine.....	30
9.3 Bone marrow transplant.....	31
9.4 Emergency management.....	31
9.4.1 VOC management:.....	31
9.4.2 ACS management:.....	32
10 Discussion and future directions.....	32
Chapter 2:.....	35
Lipid Biomarkers and Embryo Quality in In Vitro Fertilization; Pregnancy Success Differentially Expressed by Body Weight.....	35

Lipid Biomarkers and Embryo Quality in In Vitro Fertilization; Pregnancy Success Differentially Expressed by Body Weight.....	36
Abstract:.....	37
Introduction.....	38
Materials and Methods	41
Results.....	48
Discussion	65
Bibliography.....	77
Supplementary appendix:.....	100

Table of Tables:

Table 1: SCD genotype, severity of complication, region, effected ethnicities, and percent of normal hemoglobin for each type:	12
Table 2: Annual estimation of SCD patient according to WHO ¹ :.....	15
Table 3: Research terms used for the literature review:	18
Table 4: Complications of SCD and a summary of the main characteristics.....	33
Table 1. Demographic and Baseline characteristics shows the similarities between normal weight women (not obese) and obese women.....	49

Table of Figures:

Figure 1 – Pathophysiology of SCD.....	10
Figure 2: Probability of gene inheritance in SCD.....	11
Figure3: Number of newborns with SCA in 2010	16
Figure: 4 PRISMA Flow Diagram.....	21
Figure 1: Statistical analysis workflow.....	48
Figure2: Metabolites model for 2PN acquired from PPP sample.....	53
Figure 3: PL model for 2PN acquired from FF sample.	54
Figure 4: rLDA of 6-weeks of pregnancy and EHR.	57
Figure 5: rLDA of 6-weeks of pregnancy and metabolites acquired from PPP.	59
Figure 6: rLDA of 6-weeks of pregnancy and lipids without GL species acquired from FF sample.	60
Figure 7: Final model for BMI from EHR data and PPP small molecules.....	64
Figure 8: Final model for BMI from EHR data and FF small molecules.....	65

Chapter 1:

Sickle cell disease associated lipid changes and their relevance towards the disease pathogenesis: Literature

Review

Sickle cell disease associated lipid changes and their relevance towards the disease pathogenesis: Literature Review

Suad Alshammari^{1,2}, Monther Alsultan^{1,3}, Joshua Morriss¹, Silas Contaifer¹, Daniel Contaifer¹,
Wally R. Smith, Donald F. Brophy and Dayanjan S Wijesinghe^{1,4,5}

¹ Department of Pharmacotherapy and Outcomes Sciences, School of Pharmacy,
Virginia Commonwealth University, Richmond, Virginia, USA.

² Faculty of Pharmacy, Northern Border University, Saudi Arabia.

³ College of Clinical Pharmacy, King Faisal University, Saudi Arabia

⁴ Da Vinci Center, Virginia Commonwealth University, Richmond, Virginia, USA

⁵ Institute for Structural Biology Drug Discovery and Development (ISB3D), School of
Pharmacy, Virginia Commonwealth University, Richmond, Virginia, USA

Abstract

Sickle cell disease (SCD) is a group of genetic disorder that occurs due to genetic mutation of a beta-globin gene that lead to production of pathogenic hemoglobin S (Hb S). Genotypes of SCD include Hb SS (sickle cell anemia) which is the most common and severe form of SCD affects about 20 to 25 million people worldwide, HbSC, Hb S β + thalassemia, and Hb S β 0-thalassemia. SCD is characterized by multiorgan complications that, in turn, affect lipids composition. During hypoxia a sequence of changes will take place such as HbS polymerization, erythrocyte rigidity and stickiness, and oxidative stress. The combination of these changes will affect lipids components such as polyunsaturated fatty acids (PUFA), which are substrates for a

significant number of bioactive lipids such as the eicosanoids and some of the endocannabinoids. For example, vaso-occlusion crisis, the most common cause of SCD hospitalization, is found to be accompanied by changes in PUFA components of RBCs cell membrane encompassing Omega-3 and Omega-6. This comprehensive review outlines lipid changes that accompany SCD and also identify the gaps in our knowledge. This review will also allow us to devise better treatment options to manage the different pathophysiology and complications of SCD.

Introduction

1 Background

Sickle cell disease (SCD) is a group of genetic disorders^{1,2}. It is caused by genetic mutation in the beta-globin gene which results in the production of abnormal hemoglobin S (HbS), or the HbS trait³. According to the World Health Organization (WHO), 20-25 million cases of global SCD are of the homozygous HbSS subtype. The vast majority of these cases are located in sub-Saharan Africa, accounting for approximately 12-15 million people, with India as a close second of nearly 5-10 million cases⁴.

The biochemical variations that accompany the SCD mutation are numerous. Among such variation are expected difference in the lipidome. Lipidomics is a field concerned with investigating the roles lipids have in various diseases; the primary functions of lipids include them serving as energy reservoirs, signaling molecules, and to compartmentalize (via membrane formation) various biochemical reactions^{5,6}. Understanding the structures and functions of these molecules can allow for a better understanding of pathways that underly any given disease or injury. For example, the high oxidative stress caused by sickle cell disease may result in a high degree of oxidation of polyunsaturated fatty acids (PUFAs), which are substrates for a significant number of bioactive lipids such as the eicosanoids⁷. Despite more apparent metabolic modulations, the lipidome has not been studied in detail with respect to SCD. Here we outline what is known to

date with regards to the lipid and metabolic changes that accompany SCD, and also identify the gaps in the current literature with respect to these topics. A better understanding of the lipid and metabolic changes accompanying SCD will allow us to devise better treatment options to manage the different pathophysiology of SCD.

2 Pathophysiology

At the molecular level, normal hemoglobin (Hb) consists of two α and two β chains genetically coded by genes on chromosomes 16 and 11. When a mutation occurs on chromosome 11, the nitrogen base adenine codon (GAG) is substituted by thymine (GTG) leading to replacement of glutamic acid (hydrophilic) to valine (hydrophobic) in position 6 of the globin's β chain n-terminal end. The ultimate result of this process is the formation of pathogenic HbS⁸. During hypoxia, the deoxygenated HbS upregulates a long chain of insoluble polymers, causing rigidity and damage to the red blood cells (RBCs), resulting in the characteristic "sickle" shape. Furthermore, HbS gives RBCs a "sticky" property due to the secretion of adhesion molecules such as Integrin $\alpha 4\beta 1$ which interact with endothelial cells' membranes, altering the blood supply. Consequently, this affects the half-life of RBCs which is reduced to 10-20 days instead of 120 days as is the half-life of normal RBCs⁸⁻¹⁰.

A series of changes occur due to the chromosome 11 mutation (**Figure 1**). During sickling, hemolysis occurs releasing free hemoglobin into the serum, which causes calcium pump dysfunction as RBCs obtain excess Na^+ and Ca^{2+} ions with a loss of K^+ ions and water. Additionally, nitric oxide (NO) production is inhibited due to hypoxia, enabling sickle cells to stick more readily to the endothelium. Moreover, the extracellular hemoglobin interacts with NO leading to decreased nitric oxide concentration in plasma and endothelial tissue, inducing vascular complications such as vasoconstriction⁸⁻¹⁰.

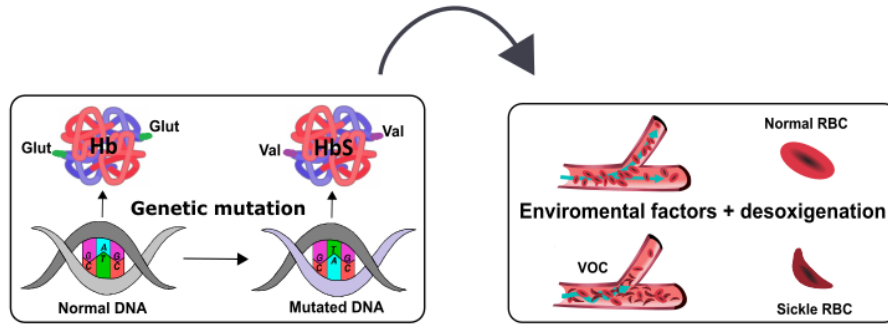


Figure 1 – Pathophysiology of SCD: a: The β globin chain mutation encoded in chromosome 11 results in substitution of adenine (GAG) by thymine (GTG), enabling the “sickled” erythrocyte. b: Under certain conditions such as those from environmental factors and hypoxia, Hbs is deoxygenated, causing long-chain polymerization which activates the sickling of erythrocyte.

3 SCD Genotypes differentiation

When a single copy HbS inherited from each of the parents leads to homozygous HbSS also known as sickle cell anemia which is a very common SCD disorder^{11,12}. Coinheritance of HbS with other pathogenic hemoglobin forms results in heterozygous classes of SCD¹². Heterozygous genotypes include hemoglobin SC (HbSC) HbS β^+ - thalassemia, HbS β^0 - thalassemia and other rare types as can be seen in **Figure 2**^{4,8}.

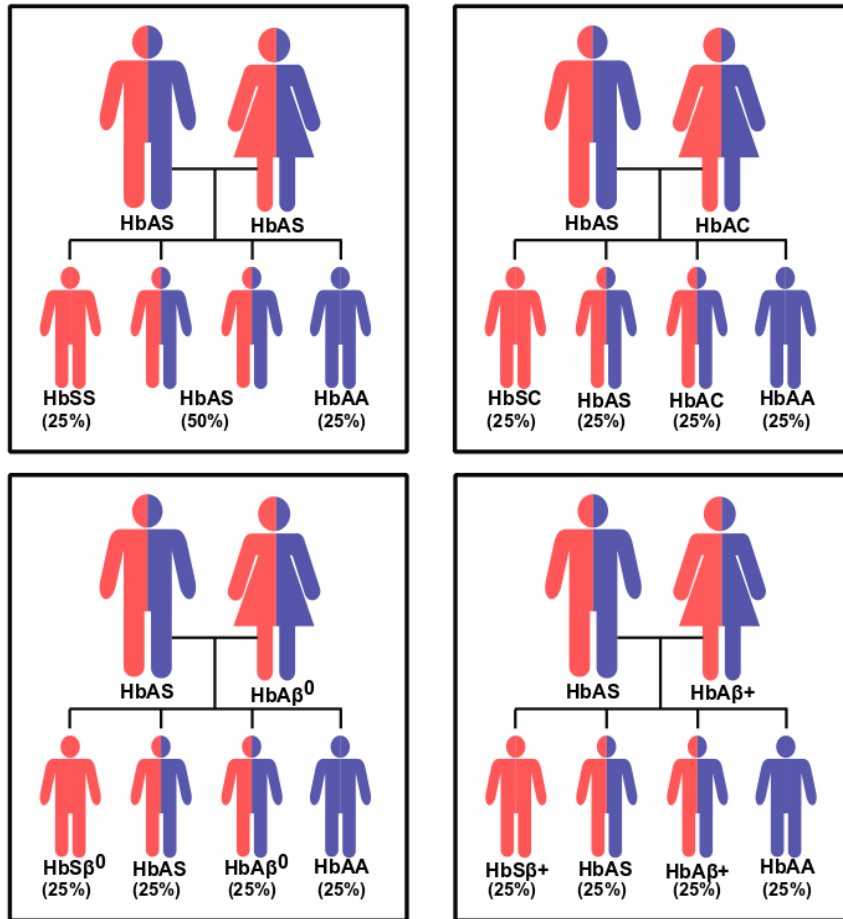


Figure 2: Probability of gene inheritance in SCD: If each of the parents carries a single copy of pathogenic hemoglobin (HbAS, HbAC, HbSβ⁰, HbSβ⁺), the probability for children to inherit the disease as follows: 25% are affected (HbSS, HbSC, HbSβ⁰, HbSβ⁺), 50% are carriers (HbAS, HbAC, HbSβ⁰, HbSβ⁺), and 25% are normal (HbAA).

One of the main consequences of SCD is the onset of anemia. Anemia is caused by reduction in hemoglobin (Hb) concentration level. The short lifespan of RBCs in SCD, again approximately 10-to-20 days in contrast to 120 days for healthy individuals, causes a decreased number of RBCs and prompts a reduction in oxygen delivery to tissues (anemia). Hb in healthy individuals have either HbA, HbA2 and HbF genotypes, usually maintaining oxygen homeostasis

throughout the body. However, sickle cell anemia (SCA) incurred by the inherited HbS gene is associated with different sub-genotypes: HbSS(Sickle Cell Anemia), HbSC, HbSβ⁰ thalassemia, HbSβ⁺ thalassemia, HbSα thalassemia, HbSD and HBAS (Sickle cell trait). The different genotypes, their respective phenotypes and prevalence are shown in **Table 1**.

Table 1: SCD genotype, severity of complication, region, effected ethnicities, and percent of normal hemoglobin for each type:

Genotype	Definition ¹	Severity of clinical manifestations ^{1,2}	Ethnicities or regions affected ^{1,3}	Prevalence among SCD ^{1,5}	% of normal vs abnormal Hb ^{4,6}	Reference
HbSS	Sickle Cell Anemia homozygous for S globin ¹⁻⁴	Severe or moderately severe and associated with shortest survival duration	70% of African ancestry	74-76%	HbA2:<3.5% HbF:5-15% or higher in rare cases	1,2,3,4
HbSC	Double heterozygous for HbS and HbC	Moderate severity	25%-30% of African ancestry	18-24%	HbA2:<3.5% HbF:1-5% or higher in rare cases	1,2,3,4
HbSβ ⁰ Thalassemia	Double heterozygous for HbS and β ⁰ Thalassemia	Severe and indistinguishable from SCA	Most common among Middle eastern and Indian ancestry	1-6%	HbA2:<3.5% HbF:2-15% HbS:80-92%	1,2,3,4

HbSb+ Thalassemia	Double heterozygous for HbS and b+ Thalassemia	Mild to moderate and varies among different ethnicities	Most common among those of Middle eastern and Indian ancestry	1-6%	HbA:3-30% HbA2:>3.5% HbF:2-10% HbS:65-90%	1,2,3,4
HbSa Thalassemia	Double heterozygous for HbS and a Thalassemia	Mild to moderate and varies based on type of thalassemia inherited	30% in African region 50% in Middle Eastern 50% of Indian ancestry	N/A	N/A	1,2,3,4,5
HbSD	Double heterozygous for HbS and HbD	Severe symptoms	Most common in those of Northern Indian ancestry	<1%	HbA2: 3.8% HbF:4.5% HbS:42.5% HbD:42.6	1,2,3,6
HbS/HPFP	HbS and hereditary persistence of fetal Hb	Very mild or not symptomatic due to high HbH	Reported in different ethnicities and multiple regions worldwide	N/A	HbA2: 2.5% HbF:10-40%	1,2,3,4,5
HbS/HbE syndrome	Double heterozygosity for HbS and HbE	Very mild symptoms or sometimes similar to HbSb+ Thalassemia	Southeast Asian ancestry	N/A	HbE:<30%	1,2,3,4,5

HbAS	Sickle cell trait A combination of a single HbS with normal Hb	No symptoms	AA-7 to 10% Sub-Saharan African ancestry 20% Latino ancestry:0.2-6.3 % Indian ancestry: 13% Middle Easter ancestry:0.2-27% Grecian ancestry: 4-10 %	Not considered a form of SCD	HbA:50-60% HbA2:<3-30% HbF:<2% HbS:36-45%	1,2,3,4,5
Other rare phenotypes combinations	Abnormal combination of HbS with HbD Los Angeles, G-Philadelphia or HbO Arab	Very rare combinations and clinical symptoms and may develop with severe hypoxia	Very rare	N/A		1,2,3,4,5

1.Saraf SL, Molokie RE, Nouriaie M, et al. Differences in the clinical and genotypic presentation of sickle cell disease around the world. *Paediatr Respir Rev.* 2014;15(1):4-12. doi:[10.1016/j.prrv.2013.11.003](https://doi.org/10.1016/j.prrv.2013.11.003)

2.Habara A, Steinberg MH. Minireview: Genetic basis of heterogeneity and severity in sickle cell disease. *Exp Biol Med (Maywood).* 2016;241(7):689-696. doi:[10.1177/1535370216636726](https://doi.org/10.1177/1535370216636726)

3.Rees DC, Williams TN, Gladwin MT. Sickle-cell disease. *The Lancet.* 2010;376(9757):2018-2031. doi:[10.1016/S0140-6736\(10\)61029-X](https://doi.org/10.1016/S0140-6736(10)61029-X)

4-Hemoglobinopathy patterns - UpToDate. Accessed July 7, 2020. https://www.uptodate-com.proxy.library.vcu.edu/contents/image?imageKey=HEME%2F116210&topicKey=HEME%2F7115&search=Overview%20of%20variant%20sickle%20cell%20syndromes&rank=1~150&source=see_link

5-Sickle cell trait - UpToDate. Accessed July 14, 2020. https://www.uptodate-com.proxy.library.vcu.edu/contents/sickle-cell-trait?search=Overview%20of%20variant%20sickle%20cell%20syndromes&topicRef=7115&source=see_link

6-Shanthala Devi AM, Rameshkumar K, Sitalakshmi S. Hb D: A Not So Rare Hemoglobinopathy. *Indian J Hematol Blood Transfus.* 2016;32(Suppl 1):294-298. doi:10.1007/s12288-013-0319-3

4 Global burden of SCD:

Globally, SCD is common in countries where malaria is widespread¹³. Annually, 275,000 to 300,000 children are born with SCD about 75% to 85% of them occur in Africa (Table2)^{13,14}. However, these numbers are expected to reach 400,000 births/year by 2050¹³. Regarding the survival rate, in developed countries, children with SCD survive to adolescence. Whereas, in developing countries, the mortality rate among children with SCD is higher. For example, in Africa, 50% to 80% of children with SCD die before five years old of age and 16.5% in West Africa (Aygun & Odame, 2012).

Table 2: Annual estimation of SCD patient according to WHO¹ :

Region	Number
African region	233,289
American region	9,047
Eastern Mediterranean region	6,491
European region	1,292

South–east Asian region	26,037
Western Pacific region	13
World	276,168

1. Aygun, B., & Odame, I. (2012). A global perspective on sickle cell disease. *Pediatric Blood & Cancer*, 59(2), 386–390. <https://doi.org/10.1002/pbc.24175>

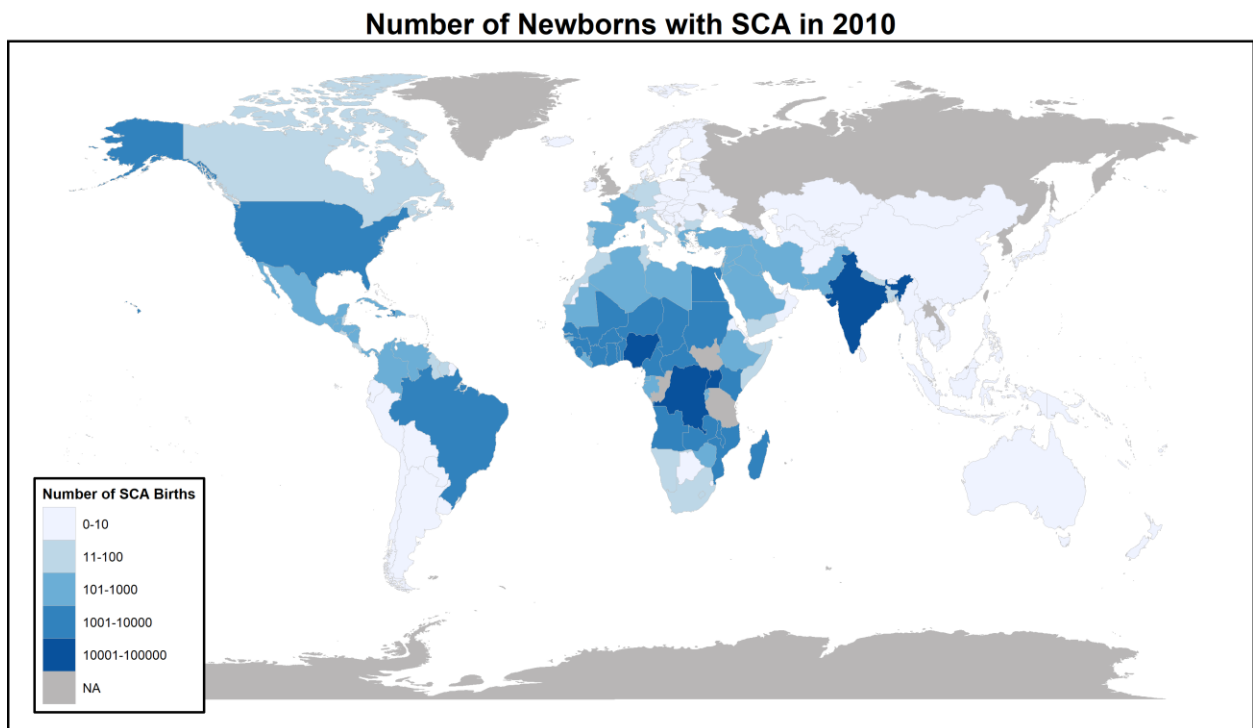


Figure3: Number of newborns with SCA in 2010. The figure is reproduced using ¹⁵ data by R software version (3.6.3).

5 SCD cell Disease in Saudi Arabia and the U.S

SCD is one of the most prevalent genetic disorders in Saudi Arabia. It was detected for the first time in the Eastern province in the 1960s. This discovery initiated multiple screening

investigations across different regions of Saudi Arabia to determine the impact of SCD. The prevalence of SCD among the Saudi population is still not fully understood. However, the Premarital Screening Program (PSP) from 2004 to 2005 reported that nearly 4.2% of screened adults carried the HbS gene, or exhibited the SCD trait, and 0.26% of the total population had SCD. For thalassemia, 3.22% carried the trait and 0.07% were affected ¹⁶. Another study conducted in 2011 suggested that somewhere between 2% to 27% of the Saudi population carry SCD trait ¹⁷. Nonetheless, newborn screening for SCD is absent in Saudi Arabia and, therefore, the true prevalence is likely underestimated.

In the U.S, the sickle cell trait (SCT) differs greatly across states, between different ethnicities and races. It is likely that many SCT carriers in the United States are not aware of their medical sickle cell condition due to the mildness of symptoms. Thus, the exact number of cases in the U.S is unspecified¹⁸. However, it has been estimated that roughly 100,000 American are affected with SCD ¹⁹. Additionally, approximately 15.5 out of every 1000 American births have been speculated to have SCD, of which the group with the highest prevalence were African Americans representing 73.1 cases per 1000 births ¹⁸. In 2004, the average hospitalization with underlying SCD-related complications reached 83,149 with a cost of roughly \$488 million ²⁰.

6 Clinical manifestation and complication of SCD

SCD is pervasive by its multisystem effects that are a result of vaso-occlusion (VOC). These effects include acute pain crises and chronic complications. VOC occurs as a consequence of sickled RBCs and the short life cycle of erythrocytes. Damaged erythrocytes block the blood supply in small vessels leading to VOC and organ damage¹⁹. Although VOC's acute pain crisis is the most common SCD complication that results in hospitalization²¹, chronic complications often come from VOC including cardiovascular, pulmonary, nervous, gastrointestinal, musculoskeletal, urogenital, spleen and systemic inflammation ¹⁹. These complications can vary across each

patient, and could range from mild to severe problems ⁴. Even though some complications can be improved with current therapeutic interventions, such as pain crisis and leg ulcers, there is little to no evidence supporting the improvement in other more chronic, end-stage complications like renal dysfunction ⁴.

The SCD complications' severity can varies among haplotypes and coinheritance of fetal hemoglobin (HbF) and α -thalassemia. HbF, found in newborns, has a higher affinity to carry oxygen than normal adult Hb $\alpha_2\beta_2$; thus, SCD-related symptoms start to emerge after six months postpartum, when HbF levels decline. It has been demonstrated that individuals with homozygous SCD in the Saudi-Indian haplotype have a high level of HbF, exhibiting reduction in SCD complications as a result of the decrease in HbS polymerization rate. Another genetic modifier that impacts the manifestation of SCD complications is the coinheritance of α -thalassemia ^{4,22}. Coinheritance of α -thalassemia incurs a reduction in the HbS polymerization rate, which leads to an increase in Hb concentration and the RBCs' lifespan ²². Also, it reduces hemolysis of RBCs leading to decrease in some complications like stroke and leg ulcers. Despite these advantages, α -thalassemia increases the progression of other complications such as pain crisis and acute chest syndrome ²².

7 Method:

We acquired the studies by searching in PubMed. In the beginning, we searched using two terms (sickle cell and lipidome), and we get only 9 publications. After that, we tried to expand our research terms by using the disease name, lipid types, and the complications of our interest. The detailed terms are represented in table 3.

Table 3: Research terms used for the literature review:

Database	Terms
PubMed	<p>(((("sickle"[All Fields] OR "sickled"[All Fields] OR "sickles"[All Fields] OR "sickling"[All Fields]) AND ("cells"[MeSH Terms] OR "cells"[All Fields] OR "cell"[All Fields]) AND ("fatty acids"[MeSH Terms] OR ("fatty"[All Fields] AND "acids"[All Fields]) OR "fatty acids"[All Fields] OR ("glycerolipid"[All Fields] OR "glycerolipids"[All Fields]) OR ("glycerophospholipids"[MeSH Terms] OR "glycerophospholipids"[All Fields] OR "glycerophospholipid"[All Fields]) OR ("sphingolipids"[MeSH Terms] OR "sphingolipids"[All Fields] OR "sphingolipid"[All Fields]) OR ("sterolic"[All Fields] OR "sterols"[MeSH Terms] OR "sterols"[All Fields] OR "sterol"[All Fields]) OR ("prenol"[Supplementary Concept] OR "prenol"[All Fields] OR "prenols"[All Fields]) OR "saccharolipids"[All Fields] OR ("polyketides"[MeSH Terms] OR "polyketides"[All Fields] OR "polyketide"[All Fields]))) AND ("acute chest syndrome"[MeSH Terms] OR ("acute"[All Fields] AND "chest"[All Fields] AND "syndrome"[All Fields]) OR "acute chest syndrome"[All Fields] OR ("vasoocclusion"[All Fields] OR "vasoocclusive"[All Fields]) OR "vaso-occlusive"[All Fields] OR ("vasoocclusion"[All Fields] OR "vasoocclusive"[All Fields]) OR "Vaso-occlusion"[All Fields] OR ("blood coagulation"[MeSH Terms] OR ("blood"[All Fields] AND "coagulation"[All Fields]) OR "blood coagulation"[All Fields]) OR ("thrombin"[MeSH Terms] OR "thrombin"[All Fields] OR "thrombin s"[All Fields] OR "thrombine"[All Fields] OR "thrombins"[All Fields]) OR ("hypercoagulant"[All Fields] OR "hypercoagulative"[All Fields] OR "thrombophilia"[MeSH Terms] OR "thrombophilia"[All Fields] OR "hypercoagulability"[All Fields] OR "hypercoagulable"[All Fields] OR "hypercoagulation"[All Fields]))) NOT ("proteom"[All Fields] OR "proteome"[MeSH Terms] OR "proteome"[All Fields] OR "proteomes"[All Fields] OR "proteomical"[All Fields] OR "proteomically"[All Fields] OR "proteomics"[MeSH Terms] OR "proteomics"[All Fields] OR "proteomic"[All Fields] OR ("covid 19"[All Fields] OR "covid 19"[MeSH Terms] OR</p>

"covid 19 vaccines"[All Fields] OR "covid 19 vaccines"[MeSH Terms] OR "covid 19 serotherapy"[All Fields] OR "covid 19 serotherapy"[Supplementary Concept] OR "covid 19 nucleic acid testing"[All Fields] OR "covid 19 nucleic acid testing"[MeSH Terms] OR "covid 19 serological testing"[All Fields] OR "covid 19 serological testing"[MeSH Terms] OR "covid 19 testing"[All Fields] OR "covid 19 testing"[MeSH Terms] OR "sars cov 2"[All Fields] OR "sars cov 2"[MeSH Terms] OR "severe acute respiratory syndrome coronavirus 2"[All Fields] OR "ncov"[All Fields] OR "2019 ncov"[All Fields] OR (("coronavirus"[MeSH Terms] OR "coronavirus"[All Fields] OR "cov"[All Fields]) AND 2019/11/01:3000/12/31[Date - Publication])) OR ("antibodie"[All Fields] OR "antibodies"[MeSH Terms] OR "antibodies"[All Fields] OR "antibody s"[All Fields] OR "antibodys"[All Fields] OR "immunoglobulins"[MeSH Terms] OR "immunoglobulins"[All Fields] OR "antibody"[All Fields]) OR ("protein s"[All Fields] OR "proteinous"[All Fields] OR "proteins"[MeSH Terms] OR "proteins"[All Fields] OR "protein"[All Fields])) AND (fha[Filter])

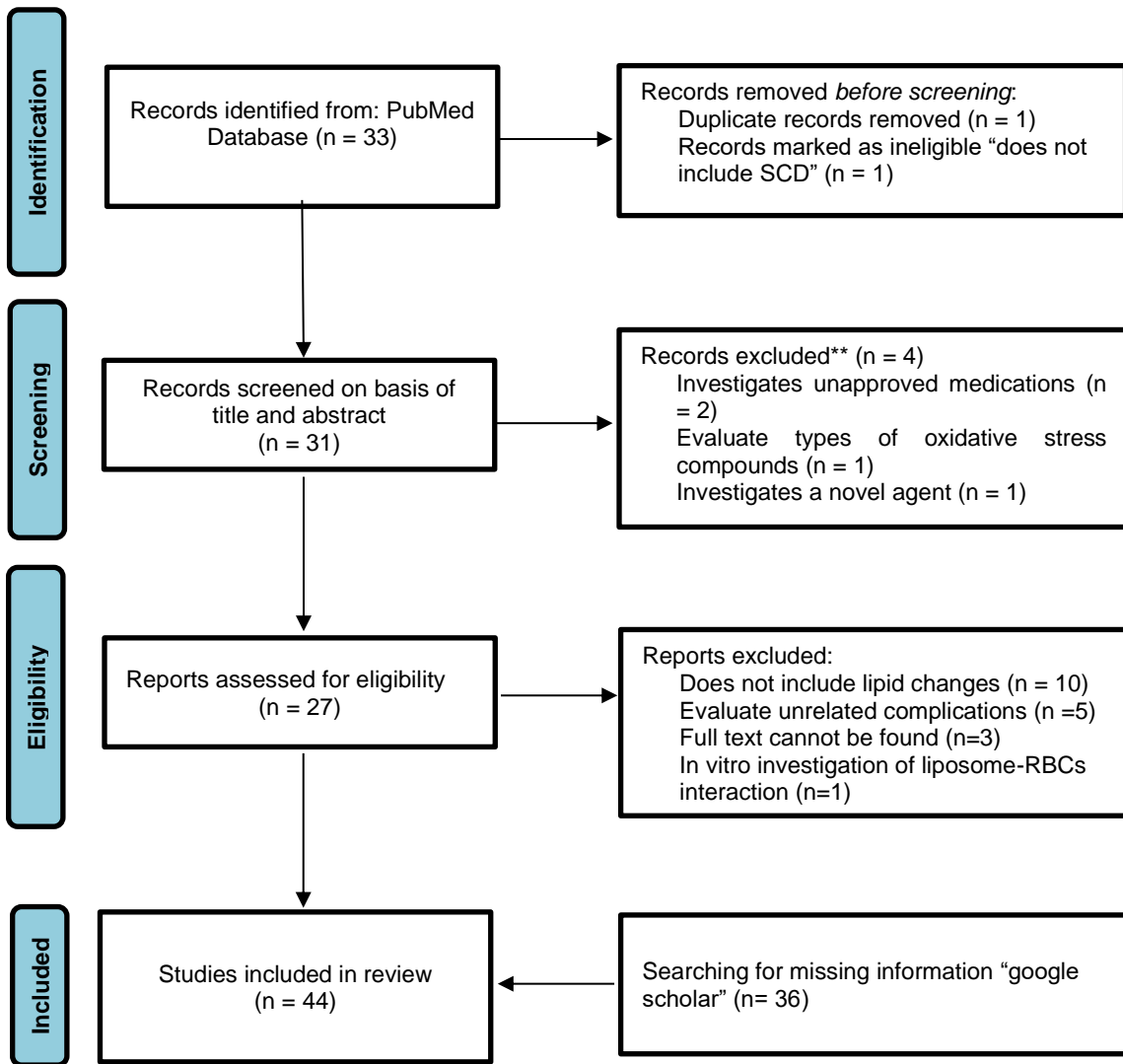


Figure: 4 PRISMA Flow Diagram.

In PubMed, the search generated 33 articles. The duplicated and irrelevant articles were excluded. After that, the titles and abstracts were reviewed. The article that was investigated unapproved medications, evaluated types of oxidative stress compounds, and investigated a novel agent were excluded. We also exclude articles that do not include lipid changes and evaluate unrelated complications. We searched for additional articles manually using “google scholar”. This search method is limited to lipids changes in sickle cell disease (not include the introduction, background, and disease burden sections).

8 Clinical manifestation and changes on lipidome in SCD

8.1 Pain and VOC

VOC acute pain is the most common cause of SCD hospitalization ²¹. Pain episodes vary from one patient to another according to stress, physical, and physiological conditions ^{23,24}. In SCD, the mechanism of pain is more complicated than the pain mechanisms in other diseases due to an involvement of multiple factors ²¹. These factors include HbS polymerization and adhesion molecules; HbS polymerization leads to RBC sickling, the release of inflammatory mediators, mast cell activation, and the release of endothelial factors; adhesion molecules, from both red and white blood cells ^{21,23,24}. During the VOC pain crisis, the accumulation of inflammatory mediators leads to nociceptor activation^{23,24}. For example, increased interleukin-1 (IL-1) is associated with elevated prostaglandins E2 (PGE2) and I2 (PGI2) synthesis which, in turn, causes nociceptor activation, inducing nerve fiber damage and pain ²⁴. Prostaglandins have also been found to affect signaling pathways that cause hyperalgesia -increase pain sensation- ²⁵. The enzyme cyclooxygenase-2 (COX-2) converts fatty acid arachidonic acid (AA) to prostaglandin E2 (PGE2), and oxidizes endocannabinoids 2-arachidonoylglycerol (2-AG) into prostaglandin glycerol esters (PG-Gs) and anandamide into prostaglandin ethanolamides (prostamides), respectively²⁵.

HbS polymerization affects the RBC membrane. In SCD, there is an elevation in phosphatidylserine (PS) expression both extra-and-intra-cellularly. According to van Tits et al. (2009), there is a greater increase in PS levels and coagulation factors during pain crises. PS contributes to VOC episodes through the activation of endothelial cells and causes adhesion of damaged (sickled) RBCs. In addition, secretory phospholipase A2 causes PS hydrolysis, which in turn leads to thromboxanes and prostaglandins generation, subsequently incurring the onset of acute chest syndrome– the leading cause of SCD deaths ²⁶. PS has a role in shortening the lifespan of RBCs. Besides PS, there are also changes in the polyunsaturated fatty acid (PUFA)

components of RBCs' cell membranes. Altered PUFAs include increase AA 20:4n-6, adrenic acid (22:4n-6), and osbond acid (22:5n-6) with decreased linoleic acid (LA, 18:2n-6), EPA (20:5n-3), and DHA (22:6n-3)²⁷⁻²⁹. These changes may participate in VOC by facilitating RBCs-endothelial interaction²⁹. Daak et al. demonstrated the efficacy of omega-3 fatty acid supplementation in HbSS patients, as they found a reduction of hospitalizations pertaining to SCD pain and VOC in patients that were administered EPA and DHA supplements²⁹. In addition, during VOC, there is an elevation in thromboxane B2 and 6-keto-prostaglandin F_{1α} (6kPGF_{1α}). This finding reflects the imbalance between vasoconstrictor and vasodilator in SCD patients³⁰.

Opioids are the most commonly used analgesics for the management of both acute and chronic pain in SCD^{23,31}. Although morphine is the first-choice opioid for pain management in SCD, it causes mast cell activation³¹, and this leads to hyperalgesia^{23,31}. In addition, morphine causes tolerance, respiratory depression, and nephropathy²³. In pain conditions not pertaining to SCD, persistent long-term opioid use leads to opioid receptors adaptation, efficacy reduction, and pronociceptive neurotransmitters activation (pronociceptive neurotransmitters have a contrary action of opioids analgesic effects). The neural adaptation to opioids is extremely complex and encompasses multiple pathways, such as activation of calcitonin gene-related peptide (CGRP) and neuropeptide substance P (sP), as well as downstream messengers derived from the aforementioned AA metabolism through cyclooxygenase (COX), lipoxygenase (LOX) and endocannabinoid pathways. During acute opioids treatment, sensory transmitters are inhibited, causing partial analgesia. In chronic opioids use, the secretion of CGRP and sP are increased; also, there is postsynaptic activation of CGRP, NK-1, N-methyl-d-aspartate (NMDA) receptors, coinciding with the synthesis of PGs through cyclooxygenase pathways, and lipoxygenase metabolites (LT) through lipoxygenase pathways³².

New strategies have been considered to reduce these side effects and increase efficacy by using adjuvant drugs or nutrients³³. One of these strategies involves combining morphine with omega-3 fatty acids^{33,34}. Omega-3 fatty acids such as EPA and DHA have anti-inflammatory and

antinociceptive effects. This antinociceptive effect provides a new strategy to prevent and treat chronic pain in several diseases, and may improve the efficacy and reduce its side effects ^{33,34}. A study conducted on male Wistar rats demonstrated analgesic and antinociceptive effects of omega-3 after 16 days of administration. In addition, using omega-3 fatty acid in combination with morphine induced the antinociceptive effect in both acute and chronic morphine use as well as reduction of tolerance in chronic morphine treatment. Furthermore, when used with omega-3 fatty acids, morphine's analgesic effects were compounded despite administration with a sub-therapeutic dose ³⁴. The mechanism of omega-3 fatty acid supplementation producing antinociceptive is still poorly understood. However, it could be through (i) inhibition of the AA cascade, which leads to blocking the production of pro-inflammatory eicosanoids and cytokines, or (ii) through the production of E-series (RvE1, RvE2) and D-series (RvD1, RvD2) resolvins from EPA and DHA as precursors that have potent analgesic actions ^{33,34}. This combinational therapy to our knowledge has not been tested in humans to treat SCD-linked pain and VOC. However, contrary to previous findings, Matte et al. (2019) evinced that using DHA in HbSS mice do not increase RvD1 level in plasma, eliciting the need for further study in the effects of omega 3 fatty acids³⁵.

The endocannabinoids system are another group of lipids that participate in pain regulation ^{36,37}. Some studies have suggested that increased concentrations of endocannabinoids in the peripheral nervous system leads to reduced hyperalgesia severity in chronic pain ³⁷. A study conducted on HbSS-BERK sickle mice using inhibitor of fatty acid amid hydrolase (FAAH), URB597, lead to increased anandamide in the periphery by suppressing its degradation through inhibition of FAAH, the enzyme responsible for endogenous anandamide breakdown. That lead to decreased hyperalgesia and nociceptor sensitization via anandamide binding to CB1 receptor on the nociceptor terminal ³⁷. Anandamide stimulates eryptosis at concentrations of 2.5 μ M; eryptosis is inherently enhanced in SCD mouse models ³⁸. In SCD, eryptosis stimulation may lead to anemia ³⁹.

17R-resolvin D1 (17R-RvD1) is a novel promising therapeutic used to suppress inflammation related to SCD. A study conducted on humanized mice model assessed the impairment of specialized pro-resolving lipid mediators involving resolving-D1 (RvD1) and 17R-RvD1 during hypoxia/reoxygenation ³⁵. In this *in vivo* model, coupled to an *ex vivo* model using SCD human blood, blood treated with RvD1 and 17R-RvD1 saw a reduction in the adhesion of leukocytes to tumor necrosis factor- α (TNF- α)–activated endothelial cells ³⁵. This finding was validated *in vivo* by the HbSS mice model, which revealed the efficacy of both RvD1 and 17R-RvD1 in diminishing leukocyte adhesion to the endothelial surface. This study also demonstrated the efficacy of administering 17R-RvD1 in the reduction of neutrophil adhesion and transmigration in HbSS mice model ³⁵. Since neutrophil adhesion preludes thrombus formation, which is considered the primary stage of VOC, prevention of neutrophil adhesion and transmigration will improve vaso-occlusion outcomes ³⁵.

8.2 Acute chest syndrome (ACS)

Acute chest syndrome (ACS) is a life-threatening complication characterized by chest pain, fever, breathing difficulties, and pulmonary infiltrate which is apparent in pulmonary radiographs ⁴⁰. It is the second most common cause of SCD patients' hospitalization, and one of leading cause of patient's death ⁴⁰. ACS affects approximately 40% of SCD patients ⁴¹ and is the underlying cause for nearly 25% of SCD-related deaths ⁴⁰. The main three causes of ACS are pulmonary infection, pulmonary embolization, and pulmonary infarction ^{42,43}. Indeed, pulmonary infection is considered the predominant cause of ACS ⁴². The National Acute Chest Syndrome Study assessed 671 ACS episodes for 538 SCD patients through the period of March 1993 to March 1997. The study found chlamydia infections is the most common cause for ACS episode in all age groups ⁴⁴. However, Mycoplasma and viral pneumonia were most prevalent for ACS in young children ⁴⁴. Besides infection, pulmonary embolism can induce ACS through infarcted bone marrow ⁴³. Fat emboli is produced from infarcted bone marrow and travel throughout bloodstream

to the lung and causes inflammation and ACS⁴³. In addition, pulmonary infarction participates in ACS development through adhesion of sickled RBCs to endothelial cells that leads to VOC and hypoxia⁴³.

During fat embolism, secretory phospholipase A2 (sPLA2), a potent inflammatory mediator, is upregulated followed by inflammation⁴⁵. When the upregulated sPLA2 hydrolyses phospholipids into FFA and lysophospholipids, it generates inflammatory mediators including AA. As a consequence, AA produces farther inflammatory products that encompass thromboxane, leukotrienes, and prostaglandins^{45,46}. Therefore, the remarkable elevation of sPLA2 before 24-48 hours of ACS could predict the episodes earlier in SCD patients⁴⁵.

Lipid peroxidation also play a key role in ACS mechanism. AA undergo peroxidation through noncyclooxygenase pathway to produce F2 isoprostane. A study was conducted on HbSS and HbSC patients to assess the level of F2 isoprostanes in patients' plasma during baseline, VOC and ACS. The study found a dramatic elevation (9-fold) of F2 isoprostanes concentration compared to normal volunteer and 6-fold increase compared to VOC⁴¹. In addition, F2 isoprostanes level declined after blood transfusion by 50-85%. However, transfusion leads to the incidence of bone marrow transplant rejection which is the only treatment for SCD⁴⁷.

8.3 Hyper-coagulopathy and SCD

Coagulation activation is a common phenomenon in SCD. Markers of platelet activation can be found in SCD patients, suggesting a constant hypercoagulable state. In a study of SCD patients with PHT, Ataga et al found evidence of thrombin generation by detecting elevation of markers such as high fibrin degradation product, D-dimer, Thrombin–antithrombin complex (TAT) and prothrombin fragment 1.2 (F1+2) levels, that were higher in SCD patients than control, although not statistically significant. In addition, it was found that there were high levels of markers

for platelet and endothelial activation, such sCD40L and sVCAM-1, respectively. These results indicate the intrinsic association of coagulation activation and endothelial dysfunction in SCD ⁴⁸. Elevated plasma levels of fibrinogen and whole-blood viscosity in SCD patients are also suggestive of a state of hypercoagulability. These markers have been associated with the pain crisis, suggesting a role of increased fibrinogen-mediated platelet aggregation in blood viscosity during pain crises in SCD patients ⁴⁹. This relationship was also reported by Tomer et al illustrating that pain episodes were associated with an elevation of plasma levels of F1+2, TAT, and D-dimer. They also demonstrated that frequency of pain episodes is correlated platelet procoagulant activity and plasma fibrinolytic activity ⁵⁰.

One of the main phospholipids involved in activation of coagulation is platelet activating factor (PAF). It is an acetyl-glycerol-ether-phosphorylcholine that participates in the activation of many cells such platelets, endothelial cells, neutrophils, monocytes, and macrophages. In normal conditions, it is continuously produced in low quantities by the activity of PAF acetylhydrolases ⁵¹. The involvement of PAF in SCD has been demonstrated in several studies. For example, Oh et al. found high level of endogenous PAF in the plasma of patients with SCD when compared with normal volunteers, and suggested that higher circulating level of PAF in patients with SCD during steady state may play a role in maintaining a state of inflammation and circulatory stress in microcirculation. In this study, it was also demonstrated that high levels of PAF were not caused by attenuation of PAF catabolism. Interestingly, they found that platelets are not the major source of circulating PAF and suggested that the higher plasma level of PAF results from the abnormal interaction of neutrophils and vascular endothelium with sickle RBCs ⁵².

There is evidence that the synthesis of PAF by human polymorphonuclear cells (PMN) and endothelial cells could be modulated by nitric oxide (NO) levels. Mariano et al demonstrated that blockade of NO synthesis triggers a spontaneous production of PAF by endothelium and PMN cells, enhancing PAF' synthesis induced by TNF- α and LPS ⁵³. In general, synthesis

of NO promotes vasodilatation and inhibits platelet activation, aggregation and endothelial adhesion. However, NO inactivation by cell-free plasma Hb produced by hemolysis can block the NO effect on platelets. Therefore, the interaction between hemolysis, impaired NO bioavailability, and platelet activation might contribute to thrombosis and PHT in SCD ⁵⁴. It has been suggested that SCD' patients have decreased NO reserves, probably due to low plasma levels of L-arginine (the precursor to NO), particularly during VOC, and these levels are inversely correlated with pain symptoms⁵⁵. The authors propose that the three major mechanisms of impaired NO bioavailability are decreased plasma L-arginine, consumption of NO by cell-free plasma hemoglobin, and depletion by reactive oxygen species.

A literature review on patients with SCD reported that chronically elevated PMN counts in SCD are associated with higher risk of sickle cells complication and mortality, suggesting a constant pro-inflammatory state even in the absence of an acute crisis ⁵⁶. Moreover, the review also reported a higher than normal presence of PMNs in the pulmonary microcirculation at the capillary–tissue interface in SCD patients. The importance of leukocyte-intermediated inflammation in SCD has also been reported. A study in isolated perfused lungs evinced that the release of PAF and leukotriene (LTB₄) from the activated PMN increased retention/adherence of sickled RBC. The authors argue that both PAF and LTB₄ can influence vascular permeability, cell infiltration, and PMN adhesion to vascular endothelium by causing the release of other inflammatory mediators ⁵⁷.

Other mechanisms occurring in the membrane of sickled RBC could have the potential to exacerbate the pro-coagulation state in the disease pathology. As covered previously, studies assessing the roles of erythrocyte adhesion markers in patients with SCD demonstrate that erythrocyte PS exposure in the outer side of the cell membrane is a major determinant of RBC–endothelial adhesion ⁵⁸. The authors suggest that this loss of phospholipid asymmetry could participate in SCD vaso-occlusion. Therefore, the phenomenon of PS exposure in sickled red cells could aggravate the sickle cell anemia due to enhanced activation of coagulation. This PS

exposure could also provide a negatively charged surface in RBCs facilitating the clotting cascade components contact. A study of blood from sickle cell patients demonstrated that PS positive' RBC are positively correlated with plasma levels of F1+2, D-dimers, and plasmin-antiplasmin complex, suggesting that sickle RBCs are responsible to the hypercoagulable state in SCD ⁵⁹.

An important pro-coagulant phenomenon in SCD is the osmotic RBC shrinkage due to changes on the Hb effects on osmotic pressure. The kinetic loss of osmotic pressure of sickle-cell Hb is caused by deoxygenation that dehydrate the erythrocyte and promote Hb aggregation ⁶⁰. Osmotic erythrocyte shrinkage can activate cation channels with subsequent Ca²⁺ influx and stimulation of sphingomyelinase to increase production of ceramides. Ca²⁺ and ceramide in sickled RBC are involved in change of phosphatidylserine asymmetry of the cell membrane. These mechanisms are also linked to the observation that PAF is released from erythrocytes triggered by hyperosmotic cell shrinkage. Lang et al showed that PAF in erythrocytes binds to PAFr and stimulates the breakdown of sphingomyelin with consequent production of ceramide, and that PAF activates cell shrinkage and PS exposure in the external membrane ⁶¹.

An indirect consequence of high PAF production in SCD patients is the over-expression of platelet-activating factor receptor (PAFr), and its relationship with an increased chance of bacterial infection. PAFr is a G protein–coupled receptor of the lipid chemokine PAF. The role that PAFr plays in pneumococcal invasion has been established *in vitro* and in mice' models of SCD. The proposed mechanism is that the phosphorylcholine on the pneumococcal cell wall mimics PAF and binds the bacteria to the endothelial cell membrane and also serves to insert the bacteria into the cell through PAFr uptake pathway ⁶².

9 Treatments

9.1 Hydroxyurea

The first discovery of Hydroxyurea was in 1869 by Dresler and Stein. In 1967, it was approved by the FDA as an antineoplastic agent to treat several types of tumors and leukemias. Decades later, it showed efficacy in the production of fetal Hb in SCD patients ⁶³. For that, the FDA approved it as the first medication for SCD treatment in 1998 ⁶⁴. Hydroxyurea, a ribonucleotide reductase inhibitor, ⁶⁵ leads to limiting the transformation of ribonucleosides into deoxyribonucleosides (the DNA building unit) which causes less DNA production ⁶⁶ which in turn impacts erythropoiesis process ⁶⁷. Consequently, stress hematopoiesis is prompted leading to recruitment of early erythroid progenitor cells that have ability to produce HbF ⁶⁷; however this mechanism remains to be fully understood ⁶⁸. In the term of disease outcomes, Hydroxyurea reduces the frequency of SCD complications such as VOC pain by about 50% as well as ACS and stroke ^{19,66}. Besides, it inhibits WBC and reticulocytes' production that acts as inflammatory mediators and reduces the frequency of blood transfusion by 50% ⁶⁶. In children with SCD, it shows clinical efficacy in minimizing the painful crisis, organ damage and stroke. Also, it enhances the growth and development of SCD children. The side effects of hydroxyurea are mild, and it mainly include nausea, headache, reticulocytopenia and neutropenia. Severe side effects are rare and may include cytopenia ⁶⁶.

9.2 L-glutamine

SCD patients demonstrate impairment in nicotinamide adenine dinucleotide (NAD) metabolism with decrease of the reduced NAD (NADH) to NAD ratio leading to NAD redox potential depletion ⁶⁵. In 2017, FDA approved L-glutamine for children and adults with SCA ⁶⁹. It improves the NADH:NAD ratio resulting in enhancement NAD redox potential ⁶⁵. Thus, it prevents erythrocytes sickling by the inhibition of oxidative stress, namely by its protective properties against free radicals. Also, it has been demonstrated to prevent other complications including VOC pain and reduce patient's hospitalization ⁶⁹. The therapy's side effects include

gastrointestinal effects accompanied by headache. However, hepatic and renal functions need to be further studied during medication course⁶⁹.

9.3 Bone marrow transplant

Bone marrow transplant is currently the only cure for SCD⁷⁰. Although the cure rate is more than 80%, this procedure is limited among patients due to the lack of appropriate donors, and the severe side effects brought on by the procedure itself ⁷⁰. Hematopoietic cell transplantation (HCT) outcomes are influenced by patients' condition and SCD complications. In young patient with B-thalassemia and low risk disease the survival rate shown to be 93% and the disease-free survival rate is 91%. These percentages are worsened in high risk patients and could reach 79% for survival rate and 58% for disease-free survival in sever risk patients ⁷¹.

However, HCT outcomes are influenced by several factors. Mainly, graft-versus-host disease (GVHD) causes HCT failure which promotes organ damage and death ⁷¹. Besides, some cases reported a delay in sexual organ development after HCT but the evidence was insufficient ⁷².

9.4 Emergency management

9.4.1 VOC management:

The new clinical evidence of the complication management cause elevation in survival rate of patients with acute complications. Multiple institutions published a guideline algorithms to facilitate management of acute pain due to VOC such as National Heart, Lung and Blood Institution (NHLBI) ⁷³. The complex pathophysiology of VOC causes a complexity of the management of the crisis ⁷⁴. Basically, opioids are widely used in acute VOC pain management ⁷³. Guidelines recommended intravenous (IV) or subcutaneous morphine (dose 0.1-0.15 mg/kg) within 15 to 20 minutes of patients arrival in emergency department ⁷⁵. According to NHLBI

recommendations, administration of adjuvant medications beside opiates such as sedative and antihistamine ⁷³. Also, NHLBI and other guidelines recommended further treatment for patients with inadequate pain relief ⁷³. Oral pain control medications with comparable potency of IV medications must be prescribed to discharged patients ⁷³. Guidelines also recommended the administration of oxygen to maintain oxygen saturation more than 92% ⁷³.

9.4.2 ACS management:

Before treatment of ACS, patient assessment is required. X-ray should be obtained to assess the presence of new infiltrate. Usually the upper or middle lung lobe is affected in pediatric patients while the lower lobe is impacted in adult ⁷³. The etiology of ACS includes infection (viral or bacterial) and embolism. The recommended management of ACS involves administration of broad-spectrum antibiotics and oxygen (O₂ saturation more than 95%). Also, blood transfusion may be required if the Hb level is less than baseline level by 1.0 g/dl to improve O₂ capacity ⁷⁴.

10 Discussion and future directions

SCD is characterized by severe complications that could be life-threatening such as VOC and hemolysis. A summary of the SCD complications is described in **Table 3**. The severity of complications ranges from patient to patient with regard to the disease phenotype and environmental factors. This review discussed the lipidomic changes of SCD for some complications as they are presently understood. However, there is a limited number of studies regarding lipidomic modulations in SCD, and the majority of them discuss only the HbSS type. In addition, there are limited studies that examine the lipid changes pre and post medication use. Morphine is widely used to manage VOC pain. However, due to its associated complications, new strategies have been used to reduce its side effects. Concomitant use of omega-3 fatty acids provides antinociceptive effects and increases morphine efficacy even in sub-therapeutic dosing.

Resolvins and endocannabinoids systems are also being explored as therapeutics to target and manage pain in SCD.

Table 4: Complications of SCD and a summary of the main characteristics.

Complications	Characteristics
Acute pain	<ul style="list-style-type: none"> ● The most common reason for hospitalization. ● Affects teenagers more than adults. ● May cause early death due to pain severity. ● Occurs in HbSS more than HbSC ● Its frequency decreases with high Hb F concentration. ● Managed by using opiates.
Infection	<ul style="list-style-type: none"> ● Occurs mainly in children. ● It is due to spleen impairment, micronutrients deficiency and complement activation deficiency. ● <i>S pneumoniae</i>, <i>H influenza</i>, and non-typhi <i>Salmonella</i> species are the most frequent infections. ● Prevented by using penicillin prophylaxis and immunization.
Neurological complications	<ul style="list-style-type: none"> ● Occurs due to vasculopathy. ● The most common cause of stroke in pediatric is HbSS. ● Stroke occurs as a result of blood flow dysregulation. ● 90% of stroke risk could be reduced by blood transfusion. ● Neurocognitive problems may be seen in children. ● Intracranial bleeding is more frequent in adults.

Acute chest syndrome	<ul style="list-style-type: none"> ● The second leading cause of hospitalization. ● Cause acute lungs injury. ● 13% of cases need mechanical ventilation. ● Managed by using broad-spectrum antibiotics, bronchodilators, and oxygen.
Heart disease	<ul style="list-style-type: none"> ● Involve both diastolic and systolic dysfunctions. ● Increase mortality rate. ● 13% of SCD patients have left-side heart disease.
Renal complications	<ul style="list-style-type: none"> ● In SCD patients, partial oxygen and pH decrease with an increase in osmolality in the kidneys. That leads to an increase in HbS polymerization. ● Renal infarction occurs due to vaso-occlusion. ● Early age renal dysfunction and albuminuria may occur.
Hemolysis	<ul style="list-style-type: none"> ● Most severe in HbSS phenotype. ● Occurs because NO reduction. ● Leads to other complications such as chronic anemia and PHT.
Hyper-coagulopathy	<ul style="list-style-type: none"> ● Elevation of coagulation markers in SCD patients even in steady state. ● Leads to other complications such as venous thromboembolism, ACS, PHT and stroke.

Chapter 2:

Lipid Biomarkers and Embryo Quality in In Vitro Fertilization;

Pregnancy Success Differentially Expressed by Body Weight

Lipid Biomarkers and Embryo Quality in In Vitro Fertilization; Pregnancy Success Differentially Expressed by Body Weight

^{1,2}Suad Alshammari; ^{1,3}Monther Alsultan; ¹Joshua Morriss; ¹Silas Contaifer; ¹Lama Basalelah; ¹Daniel Contaifer; Kai I. “Annie” Cheang; R. Scott Lucidi; Erin Mooney; Michelle Rhea; ^{1,4,5}Dayanjan S. Wijesinghe

¹ Department of Pharmacotherapy and Outcome Sciences, School of Pharmacy, Virginia Commonwealth University, Richmond VA 23298

² Faculty of Pharmacy, Northern Border University, Saudi Arabia.

³ College of Clinical Pharmacy, King Faisal University, Saudi Arabia.

⁴ Da Vinci Center, Virginia Commonwealth University, Richmond VA 23284

⁵ Institute for Structural Biology Drug Discovery and Development (ISB3D), School of Pharmacy, Virginia Commonwealth University, Richmond VA 23298

Please send correspondences to:

Dayanjan S. Wijesinghe, Ph.D.

Department of Pharmacotherapy and Outcome Sciences

School of Pharmacy, Virginia Commonwealth University,

PO Box 980533

Robert Blackwell Smith Bldg. Rm. 652A

Richmond, VA 23298-5048

USA

P: (804)-628-3316 F: (804)-828-0343

Email: wijesinghes@vcu.edu

Abstract:

Introduction: A common risk factor for infertility is obesity. The global rise of obesity accompanied with infertility has led to widespread adoption of assisted reproductive technologies such as in vitro fertilization (IVF) to achieve pregnancy. However, pregnancy outcomes such as embryo quality vary after IVF, possibly due to disruptions in metabolism. Previous metabolomic studies investigating embryo quality were limited to characterizing broadly lipid classes, or a few molecular lipid species. Here, we sought to determine specific circulating lipids and metabolites with matrix-specific effects that could serve as putative biomarkers of embryo quality, correlated with BMI, and predicted clinical pregnancy subsequent IVF.

Methods: Electronic health record (EHR) data, as well as lipids and metabolites obtained from follicular fluid (FF) and platelet poor plasma (PPP), were collected from women (n = 26) undergoing IVF. Lipids and metabolites were acquired via untargeted mass spectrometry. For embryo quality and BMI, we performed multiple linear regression analysis to find correlates. For 6 weeks pregnancy, we applied a linear discriminant analysis to select lipids and metabolites that allowed for group determination.

Results: Several lipids and metabolites were selected from both matrices (FF and PPP) that either outperformed models containing only EHR or added value to EHR models. In predicting embryo quality, glycerophospholipids obtained from PPP produced the best fit model. The predicted values include (LPC) 22:6 , phosphatidylcholine (PC) 16:1/22:6, and phosphatidylethanolamine-plasmalogen (PE-P) 16:0/22:6 were negatively

correlated with 2PN while Phosphatidylethanolamine (PE) 18:0/20:3, lysophosphatidylethanolamine (LPE) 18:1, PC 14:0/16:1, and PE-P 16:0/20:5 were positively correlated with 2PN (R adjusted = 0.730, RMSE = 0.329). For rLDA of 6-weeks of pregnancy, the best model was the metabolite model obtained from Platelet Poor Plasma (misclassification = 3.85%, Entropy R-squared = 0.809).

The BMI multicomponent domain model obtained from FF, LPC 18:1, PC 16:1/22:6, and malic acid were negatively associated with BMI while Fasting insulin and PC 16:0/22:4 were positively correlated with BMI values (R-square adjusted = 0.819, RMSE = 0.127). However, the combined data model for FF has the best prediction of BMI values. In this model, PE-P 16:0/22:6, aspartic acid, and fasting insulin as positively correlated variables with BMI values, whereas indole-3-propionic acid was negatively correlated with BMI (R-squared adjusted = 0.856, RMSE = 0.113).

Conclusion: High BMI is known to have detrimental effects on the development and success of pregnancy. It is also known to disrupt the endocrine pathways involved in the pregnancy process. This study provides information about metabolic signatures associated with BMI and pregnancy outcomes. Also, it shows the effect of 2PN value on embryo quality and the success of pregnancy.

Introduction

Infertility is a medical condition characterized by the inability of a couple to achieve clinical pregnancy after 12 months of regular, unprotected sexual intercourse. The prevalence of infertility for women of reproductive age is estimated to be 1 in every 7 couples, and 1 in every 4 couples, for those within Western countries and economically

developing countries respectively⁷⁶. Although the strongest negative predictor of fertility is increasing age for women, it is believed that other risk factors such as lifestyle and environmental factors contribute significantly towards the development of infertility⁷⁶.

A common risk factor for infertility is obesity, a disorder that is estimated to affect 42.1% of women, within the United States alone, who are 20 years of age or older⁷⁷.

Obesity is defined as a body mass index (BMI) ≥ 30 kg/m², characterized by excessive adiposity⁷⁸. Not only does obesity increase time to conception⁷⁹, it increases the relative risk of chronic anovulation⁸⁰, decreases the chance of spontaneous conception⁸¹, and is linked with greater odds of miscarriage⁸². A global rise in the prevalence of obesity in tandem with infertility has led to an increasing number of women to utilize assisted reproductive technologies such as in vitro fertilization (IVF) to achieve pregnancy⁸³. However, women who are obese exhibit low responses to controlled ovarian stimulation via IVF^{84,85}. Cellular and subcellular disruptions co-occurring with obesity may account for these poor reproductive outcomes subsequent to IVF.

The impact of obesity on reproductive function can be understood through aberrant endocrine signaling pathways that dysregulate the hypothalamic-pituitary-ovarian (HPO) axis, the system that drives reproduction by cyclic production of gonadotropic and steroid hormones⁸⁶. Notably, obesity exerts an inhibitory effect on gonadotropic production, and women who are obese require higher doses of administered gonadotropins such as follicle stimulating hormone (FSH) during IVF in order to achieve an ovulatory response, comparable to women of normal weights^{87,88}. Women who are obese additionally have markedly lower pulsatile luteinizing hormone (LH) amplitudes and progesterone

metabolite secretion, further implicating the HPO axis as a central mechanism for poor IVF outcomes⁸⁹. Bridging obesity with the dysregulation of the HPO axis in women who are obese is insulin resistance (IR), which is exacerbated by lipotoxicity^{90,91}.

Lipotoxicity in ovarian tissues can exacerbate IR, is a potential mechanism for oocyte organelle damage, and has the potential to induce hyperinsulinemia, which can promote obesity^{92,93}. Under euglycemic, hyperinsulinemia conditions, elevated non-esterified fatty acid (FFA) content concomitant high insulin levels can selectively impair LH and FSH, suggesting that the endocrine disruption in women who are obese may be mediated by direct lipotoxic effects on the HPO axis⁹⁴. During IVF, concentrations of FFA, triglyceride (TAG), and long-chain acylcarnitine species within follicular fluid (FF) of women who are obese are positively correlated with gonadotropin-stimulated androgen levels⁹⁵. Additionally, in the FF of women with normal BMI who failed to respond to IVF, there is a significant shift in the accumulation of monoacylglycerols (MAG) and glycerophospholipids like phosphatidylethanolamine (PE) towards triacylglycerols (TAG) and cholesteryl esters⁹⁶. Lastly, circulating levels of TAG as a total lipid class is negatively correlated with embryo quality, as determined by the presence of two clearly distinct pronuclei and two polar bodies (2PN)⁹⁷. Taken together, a diversity of lipids and metabolites dysregulated in an obese state promote a number of deleterious pathophysiological processes, and exert modulatory effects on fertility.

Yet which lipid species and metabolites are clinically relevant towards the predicting the outcomes of IVF in women who are obese remains unknown. Current clinical evidence for IVF success or failure have been methodologically limited to only a few lipid species studied, or do not associate specific lipid species with embryo quality or

fertility, only assessing lipids by their classes (i.e. total TAG). Therefore, we sought to determine specific circulating lipids and metabolites, within the plasma and FF, that could serve as putative biomarkers of 2PN, and which play a role in reduced IVF pregnancy rates associated with obesity.

Materials and Methods

1) Patients

Follicular fluid (FF), platelet poor plasma (PPP), and electronic health record (EHR) data were collected from women (n = 26) undergoing IVF. Body composition (percentage of body fat mass) was obtained by bioelectrical impedance⁹⁸. Women's weights were recorded as either normal, overweight, or obese. The study design has been previously reported (VCU IRB#: HM20004988), but in brief; starting on menstrual cycle day 3, patients self-administered gonadotropins and underwent transvaginal ultrasounds every 2 days. Blood was drawn prior to ovarian stimulation via subcutaneous injection with human chorionic gonadotropin (hCG, 250 µg), and processed into plasma, once adequate mature follicles were detected (approximately cycle day 10-12). A follow-up visit coincided 34-36 hours post hCG, where blood was drawn and FF was obtained during egg retrieval. Patients were asked to fast after midnight of the night before the baseline visit, and were provided an optional 2-hour oral glucose tolerance test to determine if they were diabetic

(GDM threshold was ≥ 140 Mg/dl)⁹⁹. Additionally, patients were asked to recall what they had eaten within the previous 24 hours prior to their follow-up visit. Whether or not pregnancy was achieved 6 weeks after IVF was recorded. Two weeks after oocyte retrieval, serum hCG was used to evaluate pregnancy and, if serum hCG was positive, an additional visit 6-weeks post hCG occurred to confirm absence or presence of pregnancy.

2) Sample Preparation and Storage

During egg retrieval, discarded FF was obtained and transferred to Heathrow 2.0 mL Screw-Top Tubes with O-Ring caps. Samples of FF were then stored at -80°C until needed for lipidomic and metabolomic analysis.

The following protocol was used to prepare PPP: whole blood (7.4 mL) was collected in K2EDTA tubes upon the patient's visit. Whole blood was then centrifuged at $1300g$ for 10 minutes using an Eppendorf centrifuge 5810 R to separate the platelet rich plasma (PRP) layer. The upper PRP layer was then collected, avoiding contamination of the buffy coat. To obtain PPP, PRP was centrifuged at $2000 g$ for 15 minutes. Samples of PPP were then aliquoted at 0.2mL into Eppendorf tubes and stored at -80°C until needed for lipidomic and metabolomic analysis¹⁰⁰.

3) Lipidomic and Metabolomic Extraction

3a) Extraction of lipids and metabolites for liquid chromatography (LC) lipidomic and metabolomic analysis

Either 20 μL aliquot of FF or PPP had their lipids, along with water-soluble metabolites, extracted by a biphasic solvent system²⁶. In detail, sample was introduced

to 225 μL of cold methanol in a 1.5 mL polypropylene tube, mixed with odd chain and deuterated lipid internal standards [lysophosphatidylethanolamine (lysoPE 17:1), lysophosphatidylcholine (lysoPC 17:0), phosphatidylethanolamine (PE 17:0/17:0), phosphatidylcholine (PC 12:0/13:0), phosphatidylglycerol (PG 17:0/17:0), sphingosine (d17:1), d7 cholesterol, sphingomyelin (SM 17:0), C17-ceramide (d18:1/17:0), d3-palmitic acid (16:0/16:0/16:0), 1-margaroyl-glycerol (MAG 17:0/0:0/0:0), 1-oleoyl-2-acetyl-sn-glycerol (DAG 18:1/2:0/0:0), 1,2-diacyl-sn-glycerol (DAG 12:0/12:0/0:0), and 1,3(d5)-diheptadecanoyl-2-(10Z-heptadecenoyl)-glycerol (d5-TAG 17:0/17:1/17:0)]. Thereafter 750 μL of cold methyl *tert*-butyl ether (MTBE) was added and vortexed, and phase separation induced by 188 μL of liquid chromatography mass spectrometry (LC-MS)-grade water. Extracts were centrifuged at 12,300 rpm for 2 minutes, with the upper organic phase (300 μL) collected for analysis of lipids, and evaporated under vacuum conditions. Resuspension occurred with 110 μL of methanol/toluene (9:1, v/v) containing 12-[(cyclohexylamino) carbonyl]amino]-dodecanoic acid (CUDA, 50 ng/ml; internal standard for quality control of injection), vortexed, and centrifuged at 800 rpm for 5 minutes. The resultant supernatant (100 μL) underwent lipidomic analysis. An aliquot (125 μL) of the lower phase was evaporated under vacuum conditions and resuspended in pure acetonitrile (ACN). These extracted metabolites were then subjected to metabolomic acquisition via hydrophilic interaction (HILIC) LC-MS/MS¹⁰¹.

3b) Extraction of metabolites for gas chromatography (GC) metabolomic analysis

Small metabolites (<650 Daltons) were acquired from 30 μL aliquots of FF or PPP added to 1.0 mL of cold extraction solution consisting of acetonitrile, isopropanol (IPA) and water (3:3:2, v/v/v)¹⁰². Samples were vortexed for 5 minutes at 4°C and centrifuged

for 2 minutes at 14,000 relative centrifugal force (rcf). A total of 450 μ L of the supernatant was dried under a cold trap concentrator and then reconstituted with 450 μ L ACN:water (50:50 v/v) solution, centrifuged for 2 minutes at 14,000 rcf, and then subjected to drying under a cold trap. Derivatization occurred with the addition of 10 μ L of 40 mg/mL methoxyamine hydrochloride solution to the dried samples and quality controls, including N-methyl-N-trimethylsilyl-trifluoroacetamide (MSTFA) and fatty acid methyl esters (FAME). Samples were shaken at 30°C for 1.5 hours, then mixed with 91 μ L of MSTFA and FAME. After shaking at maximum speed at 37°C, for 30 minutes, the contents were transferred for metabolomic acquisition via gas chromatography mass spectrometry (GCMS)²⁷.

4) Lipidomic and Metabolomic Data Acquisition

4a) LC-MS Lipidomic data acquisition

Reverse phase, untargeted analysis was performed with a Sciex TripleTOF 6600 coupled to an Agilent 1290 LC. Lipids were separated on an Acquity ultra-performance liquid chromatography (UPLC) CSH C18 column (100 \times 2.1 mm; 1.7 μ m) (Waters, Milford, MA, USA) as previously reported by our group²⁸. The column was maintained at a temperature of 65 °C with a constant flow-rate of 0.6mL/min. The mobile phases were Mobile Phase A at 60:40 (v/v) ACN:water with 10 mM ammonium acetate, and Mobile Phase B at 90:10 (v/v) IPA:ACN with 10 mM ammonium acetate. Lipid separation was conducted following a stepwise gradient program as follows: 0-2 minutes (Mobile Phase B: 15-30%), 2-2.5 minutes (Mobile Phase B: 48%), 2.5-11 minutes (Mobile Phase B: 82%), 11-11.5 minutes (Mobile Phase B: 99%), 11.5-12 minutes (Mobile Phase B: 99%), 12-12.1 minutes (Mobile Phase B: 15%), 12-14 minutes (Mobile Phase B: 15%). Negative

and positive electrospray ionization (ESI) modes were applied with nitrogen serving as the desolvation gas and the collision gas. The MS instrument parameters were as follows: curtain gas: 35; collision-induced dissociation (CAD): high; ion spray voltage: 4500V; source temperature: 350°C; gas 1: 60; gas 2: 60; declustering potential: $\pm 80V$, and a collision energy of $\pm 10^{103}$.

4b) LC-MS Metabolomic data acquisition

Detection of water-soluble PPP and FF metabolites underwent separation via normal phase LC on a Sciex TripleTOF 6600 coupled to Agilent 1290 LC¹⁰³. Metabolites were separated by an Acquity UPLC BEH Amide (130Å, 1.7 μm , 2.1 mm X 150 mm) column (Waters, Milford, MA, USA). Column temperature was maintained at 45°C at a constant flow-rate of 0.4 mL/min. Two mobile phases were utilized, consisting of Mobile Phase A, which was LC-MS grade water with 10 mM of ammonium formate and 0.125% formic acid, and Mobile Phase B at 90:10 (v/v) ACN:water with 10 mM of ammonium formate and 0.125% formic acid. Analytes were separated using a stepwise gradient program as follows: 0–2 minutes (Mobile Phase B: 100%), 2–7.7 minutes (Mobile Phase B: 70%), 7.7–9.5 minutes (Mobile Phase B: 40%), 9.5–10.25 minutes (Mobile Phase B: 30%), 10.25–12.75 minutes (Mobile Phase B: 100%), 12.75–16.75 minutes (Mobile Phase B: 100%). Injection volumes were 1 μL and 3 μL for the positive and negative modes, respectively. Positive and negative ESI modes utilized nitrogen serving as the desolvation gas and the collision gas, and the MS instrument parameters were: curtain gas: 35; CAD: high; ion spray voltage: 4500V; source temperature: 300°C; gas 1: 60; gas 2: 60; declustering potential: $\pm 80V$, and collision energies $\pm 10^{103}$.

4c) GC-MS Metabolomic data acquisition

Metabolites were acquired on a Leco Pegasus IV time of flight mass spectrometer, coupled with an Agilent 6890 GC that was equipped with a Gerstel automatic liner exchange system (ALEX) that had a multipurpose sample (MPS2) dual rail, and a Gerstel CIS cold injection system (Gerstel, Muehlheim, Germany)¹⁰². The transfer line was maintained at 280°C, and separation was achieved on a 30 m long, 0.25 mm i.d. Rtx-5Sil MS column (0.25 µm; 95% dimethyl 5% diphenyl polysiloxane film) with a built-in, integrated guard column (10m; Restek, Bellefonte PA) with a constant flow (1 mL/min) of helium (99.999%; Airgas, Radnor, PA, U.S.A.) as the carrier gas. The oven temperature was held constant at 50°C for 1 minute, and then ramped at 20°C/min to 330°C, which was held constant for 5 minutes. The GC temperature program was set as follows: 50°C to 275°C final temperature at a rate of 12°C/s and held for 3 minutes. The injection volume was 1 µL in splitless mode at 250°C. Electron impact ionization at 70 eV was employed with an ion source temperature of 250°C. The scan mass ranged from 85-to-500 Da with an acquisition rate of 17 spectra/second¹⁰².

5) *Statistical Analysis*

Baseline characteristics and demographic parameters were assessed for any significant ($p < 0.05$) differences that could confound our findings between women with obesity and healthy-weight women undergoing IVF. Lipidomic and metabolomic data were acquired as ratios of mass-to-charge, and were normalized by mTIC to enable the merger of these two datasets, obtained from different instruments and techniques¹⁰². Metabolic data were filtered to exclude any detected exogenous metabolites identified as products of gut microbiota so that we obtained only endogenous metabolites, relevant to the physiological response of the patient undergoing IVF. Winsorization of outliers

occurred for any value outside of 1.5 times the interquartile range¹⁰⁴, and missing values for EHR data were imputed by the median of the variable. Any missing values for the outcome measures, 6-week pregnancy (a binary of “yes” or “no”) and 2PN (nominal) were excluded. Then the data were log-transformed and pareto-scaled to correct for technical variation and other factors not attributable to induced biological variation¹⁰⁵. Phospholipids were identified by their head group, parent-fragment pair, and by their sum fatty acid composition.

An overview of the statistical analytical workflow is presented within **Figure 1**, and this analysis was performed separately for FF and PPP analytes. Four domain models were used to ascertain the most important predictors belonging to lipids, metabolites, and EHR data for our chosen outcomes. These models consisted of either strictly metabolites, EHR data, or lipids, with two models containing either with glycerophospholipids (and lysophospholipids) or excluding glycerophospholipids. We performed stepwise multiple linear regression analysis (MLRA) with forward selection of candidate predictors among EHR, lipids, and metabolites that best fit BMI and 2PN. For our binary outcome of 6-weeks pregnancy, we conducted a stepwise, regularized linear discriminant analysis (rLDA) to discriminate between pregnant and non-pregnant women. Lastly, predictors from lipids, metabolite, and EHR models were combined into a multi-component model for the final discriminant analysis model. To control for confounders, univariate models assessed whether selected predictors were also associated with confounders, and if so, the final multivariable model was fit to identify discriminatory lipids and metabolites after adjusting for potential confounders. The statistical analysis described herein was performed with JMP14Pro, MetaboAnalyst 4.0, and with R-scripts written by us.

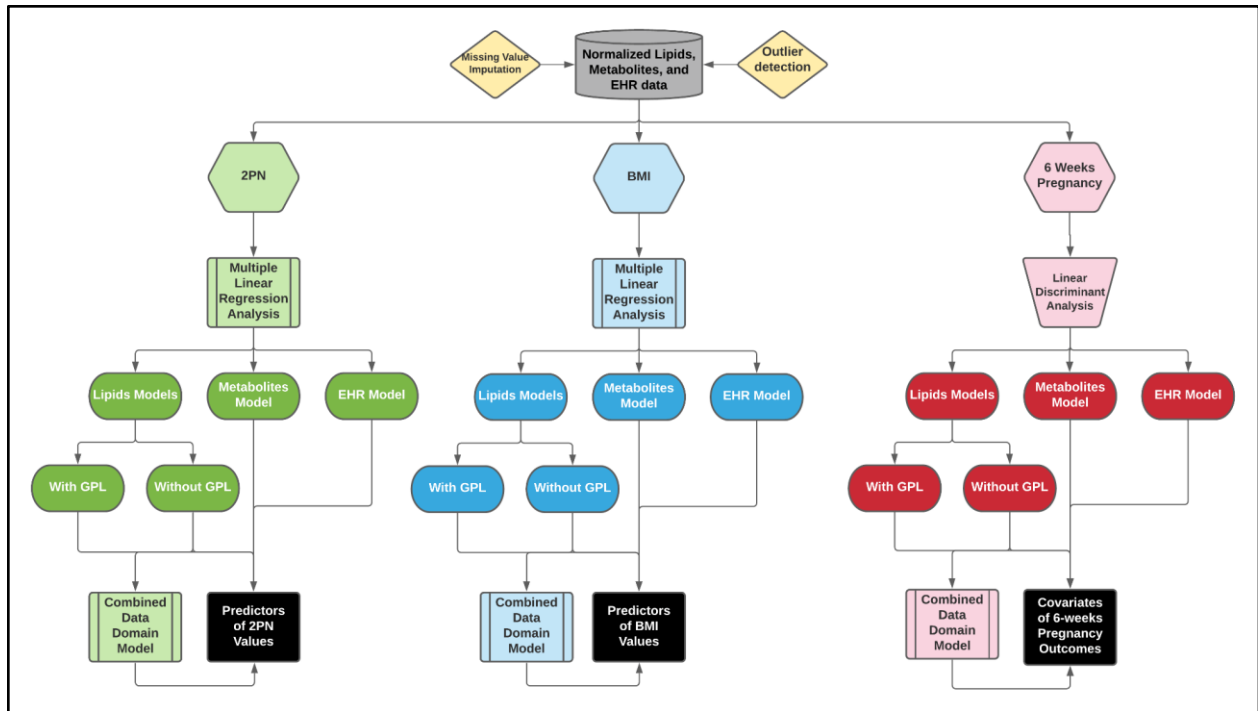


Figure 1: Statistical analysis workflow.

Results

Current clinical evidence for IVF success or failure have been methodologically limited, and this is problematic as lipids and cholesterol species in particular display high levels of compositional and functional heterogeneity. For example, cholesteryl esters, the single most abundant lipid class in human plasma and preferred form of cholesterol in lipoprotein particles, consist of several hundreds of molecular species¹⁰⁶. We sought a qualitative approach to best characterize specific lipid species and metabolites that could sufficiently determine embryo quality and predict pregnancy outcomes in women with obesity following IVF.

Characteristics of the study cohort and adjustments by Fasting Insulin

At the enrollment of this study, patients in either weight group had similar distributions of age, maximal serum estradiol, highest dosage of FSH used, total cumulative FSH used, and dietary scores (**Table 1**). T-tests at baseline determined no statistically significant ($p>0.05$) difference between demographic parameters for the treatment groups, except with BMI ($p<0.0001$), fasting insulin concentrations ($p = 0.001$), and the homeostatic model assessment for insulin resistance (HOMA-IR, $p = 0.003$). Because of this difference in insulin resistance, features selected for the final models of 2PN, BMI, and 6-weeks pregnancy outcomes were adjusted by fasting insulin concentrations. Interestingly, when considering only weight class, both obese and healthy-weight groups had similar 6-weeks pregnancy ($p = 0.229$) and 2PN ($p = 0.208$) outcomes following IVF (**Table 1**).

Table 1. Demographic and Baseline characteristics shows the similarities between normal weight women (not obese) and obese women

	Normal (n=10)	Obese (n=16)	p-value
Female age, mean (SD)	33.30(5.1)	33.99(3.2)	0.712
BMI	21.71(1.7)	34.42(9.7)	<0.0001
Fasting glucose	84.7(4.42)	87.12(7.11)	0.29
Fasting insulin	4.63(2.06)	11.01(1.53)	0.001
HOMA-IR	0.97(0.466)	2.31(1.47)	0.003
Mediterranean diet score	25.1(7.35)	22.06(1.67)	0.303

Total score black food fat screener	14.4(7.39)	17(5.93)	0.361
Total score block questionnaire fruit vegetable	13(3.43)	11.06(4.73)	0.240
Average setting	335.57(131.24)	311.51(169.62)	0.689
Cycle plan, n(%)	10(38.46)	15(57.69%)	0.318
Antagonist downreg	0(0%)	1(3.85%)	
Highest dosage of FSH used	397.5(50.62)	389.06(73.58)	0.732
Total cumulative FSH used	4327.5(1392.86)	4397.65(1375.86)	0.901
Maximal serum estradiol	1312.78(739.94)	1511.425(952.54)	0.557
6 weeks pregnancy	0.5(0.527)	0.25(0.447)	0.229
2PN	17.1(10.80)	11.68(2.34)	0.208

Note, 2PN=2 polar bodies, SD= Standard Deviation, BMI= Body Mass Index, HOMA ISI= Homeostatic model assessment Insulin Sensitivity Index. Data presented as mean (SD).

Domain Independent and multicomponent MLRA models predict 2PN values with lipids and organic compounds, differing across PPP and FF matrices

The EHR model for predicting 2PN retrieved female age in years, fasting glucose, fasting insulin, Mediterranean diet score, the total score from the block food questionnaire fat screener (23 high), the total score from the block food questionnaire fruit and vegetable screener (11 low), average sitting time as total minutes per day (test statistic = 0.665,

Prob > |t| = 0.0221), and total cumulative FSH used (test statistic = -1.44, Prob > |t| = 0.0015) as covariates, while only the average sitting time (total of minutes per day) was negatively associated with an increase in 2PN values (R adjusted = 0.769, RMSE = 0.144). From the EHR data used to construct this model, only average sitting time and total cumulative FSH used were the clinical parameters that were significant after two-way hypothesis testing. Yet in constructing the MLRA model, predictors are covaried with another, thus those that were non-significant following a two-way hypothesis test were kept within this clinical parameter model and all remaining MLRA models.

- *Metabolites acquired from PPP allowed for the best fit model across other domain models for 2PN values*

Without exclusion of PPP lipids belonging to the glycerophospholipid (PL) family, we observed the following to best predict increasing 2PN values: PL that decreased in circulating with increasing 2PN numbers were lysophosphatidylcholine (LPC) 22:6 (test statistic = -1.01, Prob > |t| = 0.0231), phosphatidylcholine (PC) 16:1/22:6, and phosphatidylethanolamine-plasmalogen (PE-P) 16:0/22:6 (test statistic = -0.899, Prob > |t| = 0.0004). Phosphatidylethanolamine (PE) 18:0/20:3, lysophosphatidylethanolamine (LPE) 18:1 (test statistic = 0.928, Prob > |t| = 0.0005), PC 14:0/16:1 (test statistic = 0.4698, Prob > |t| = 0.0060), and PE-P 16:0/20:5 (test statistic = 0.483, Prob > |t| = 0.0013) were those PL that were either positively associated or correlated with 2PN (R adjusted = 0.730, RMSE = 0.329).

Exclusion of PL and inclusion of other lipid species from our PPP model derived a model with poorer fit for 2PN (R adjusted = 0.666, RMSE = 0.365). Nonetheless, we found

the following nonesterified fatty acids (FFA) and cholesteryl esters (CE) to be associated or correlated with 2PN: those that increased with 2PN values included CE 14:0, CE 20:5 (test statistic = 0.931, Prob > |t| = 0.0236), FFA 19:1 (test statistic = 1.01, Prob > |t| = 0.0288), and myristic acid. Inversely, those that decreased corresponding a rise in 2PN values were CE 16:0, CE 22:6 (test statistic = -1.555, Prob > |t| = 0.0007), FFA 14:1, FFA 18:2, FFA 20:5, and lauric acid (test statistic = -0.771, Prob > |t| = 0.0137).

Comparatively, the metabolic model performed better against both lipid domain models and the final model (R adjusted = 0.749, RMSE = 0.317), as depicted in **Figure 2**, and included the following small molecules: 2-ketoisovaleric acid (test statistic = -0.971, Prob > |t| = 0.0001), 3-aminoisobutyric acid (test statistic = -0.611, Prob > |t| = 0.0004), beta alanine (test statistic = -0.638, Prob > |t| = 0.0007), glutamic acid (test statistic = -0.887, Prob > |t| = 0.0002), and serine (test statistic = -0.897, Prob > |t| = 0.0033) were negatively correlated with 2PN. However, those metabolites that were positively correlated with 2PN values involved aspartic acid (test statistic = 0.500, Prob > |t| = 0.0236), ornithine (test statistic = 0.683, Prob > |t| = 0.0225), and phosphate (test statistic = 0.852, Prob > |t| = 0.0030).

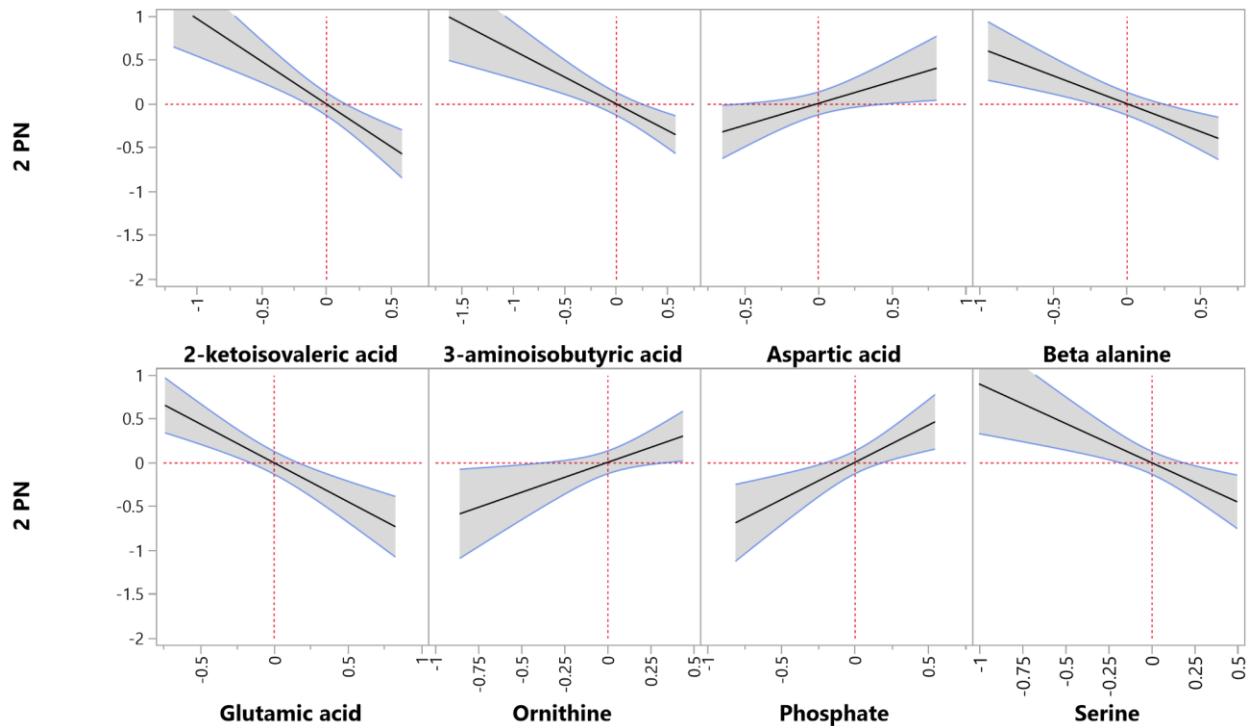


Figure2: Metabolites model for 2PN acquired from PPP sample.

When combining all data domains, the final model for PPP to predict 2PN values was constructed: positively correlated analytes included LPE 20:4 (test statistic = 0.765, Prob > |t| = 0.0023), PC 14:0/16:1 (test statistic = 0.255, Prob > |t| = 0.0329), and phosphate (test statistic = 1.03, Prob > |t| = 0.0003). Negatively correlated predictors were LPC 22:6 (test statistic = -0.652, Prob > |t| = 0.0057), CE 16:0 (test statistic = -0.595, Prob > |t| = 0.0056), and FA 20:5 (test statistic = -0.289, Prob > |t| = 0.0212). Although better fit than the lipid models (R adjusted = 0.727, RMSE = 0.331), the combined model performed worse than the PPP metabolites model for 2PN.

- Including Glycerophospholipids produced the best fit FF model for predicting 2PN values against other Lipid, Metabolic, and Combined domain models

Inclusion of PL from FF generated a model that included two acylcarnitine species as well various PLs. Acylcarnitine C16:0 (test statistic = 0.417, Prob > |t| = 0.0033), containing palmitic acid, was positively correlated with 2PN values, yet acylcarnitine C18:1 (test statistic = -0.542, Prob > |t| = 0.0358), or an L-carnitine esterified with oleic acid, was negatively correlated. Retained PL from FF that decreased with 2PN values were LPC 16:1 (test statistic = -0.853, Prob > |t| = 0.0047), lysophosphatidylinositol (LPI) 18:2 (test statistic = -1.00, Prob > |t| = 0.0023), and PC-Plasmalogen (PC-P) 18:0/22:6 (test statistic = -0.799, Prob > |t| = 0.0013). Those PL that were positively correlated with 2PN numbers were LPC 22:4 (test statistic = 0.603, Prob > |t| = 0.0028), LPE 20:4 (test statistic = 0.927, Prob > |t| = 0.0042), and LPI 18:1 (test statistic = 1.16, Prob > |t| = 0.0048). Of the FF models, this model performed the best for predicting 2PN values (R adjusted = 0.755, RMSE = 0.312), the results of which can be viewed in **Figure 3**.

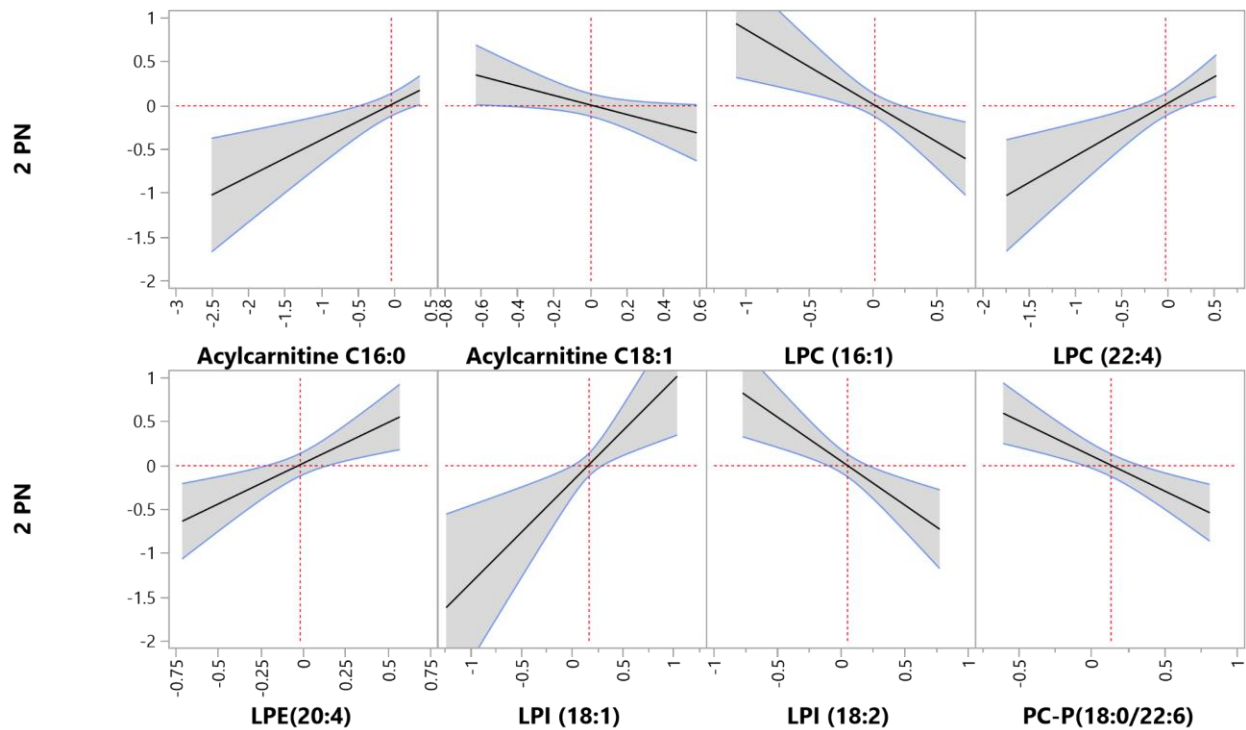


Figure 3: PL model for 2PN acquired from FF sample.

From our FF lipid model (R adjusted = 0.726, RMSE = 0.331) excluding PL, lipids that positively associated or correlated with 2PN involved CE 16:1, CE 18:1 (test statistic = 1.26, Prob > |t| = 0.0009), and arachidic acid. Among the negatively associated or correlated lipids, when excluding PL, included CE 18:3, CE 22:6 (test statistic = -0.914, Prob > |t| = 0.0003), FA 14:0 (test statistic = -0.439, Prob > |t| = 0.0410), FA 16:0 (test statistic = -0.585, Prob > |t| = 0.0410), FA 22:3 (test statistic = -0.894, Prob > |t| = 0.0003).

Metabolites acquired from FF were all negatively correlated with 2PN values, with the exception of 1-monolein, which bore a positive association with increasing 2PN. Nonetheless, the metabolites from our model included 2-aminobutyric acid (test statistic = -0.646, Prob > |t| = 0.0021), alanine (test statistic = -1.09, Prob > |t| = <0.0003), hexose (test statistic = -0.591, Prob > |t| = <0.0010), phenylalanine (test statistic = -0.908, Prob > |t| = 0.0108), and phenylethylamine (test statistic = -0.975, Prob > |t| = 0.0002). Despite the metabolites model performing better than the FF lipid model excluding PL (R adjusted = 0.7299, RMSE = 0.329), metabolites alone failed to outperform the FF lipid model including PL.

A final model with all 4 data domains gave a model without any EHR parameters (R-squared adjusted = 0.748, RMSE = 0.317). Lipids and metabolites selected were negatively correlated or associated with 2PN values except arachidonic acid containing LPE 20:4 (test statistic = 0.854, Prob > |t| = 0.0040). Remaining molecules were PC-P 18:0/22:6 (test statistic = -0.622, RMSE = 0.0115), 2-aminobutyric acid, alanine (test statistic = -0.771, RMSE = 0.0062), phenylethylamine, and FA 22:3 (test statistic = -0.429, RMSE = 0.0438).

Regularized Linear Discriminant analysis (rLDA) of 6-weeks of pregnancy

Pregnancy was discretized as a binary, categorical outcome, or as either “yes” (1) or “no” (0), 6-weeks after IVF. Ergo, the objective of these stepwise, regularized linear discriminant analytical (rLDA) models was to classify patients along this binary¹⁰⁷. EHR data alone surprisingly gave the highest rate of misclassification (19.23%) and the poorest entropy R-squared, a measure of classification quality or goodness of separation, across all of the component models (Entropy R-squared = 0.356). EHR parameters included in this model were female age, fasting glucose, Mediterranean diet score, total score block food fat screener (23 high), total score block food fruit and vegetable screener (11 low), average sitting time (total of minutes per day), total cumulative FSH used, and maximal serum estradiol value. A 95% confidence level ellipse was plotted for each canonical variables mean, pregnant or non-pregnant, as well as an ellipse denoting a 50% contour for each group, depicting a region that contains approximately 50% of the observations. The set of rays in the biplot represents the covariates, whose coefficients in the linear combination were canonical weights. Thus, the larger a covariate’s canonical weight, the greater its association with the canonical variable. The length and direction of each ray in the biplot indicates the degree of association of the corresponding covariate with the canonical variable, 6-weeks pregnant or failed pregnancy (**Figure 4**).

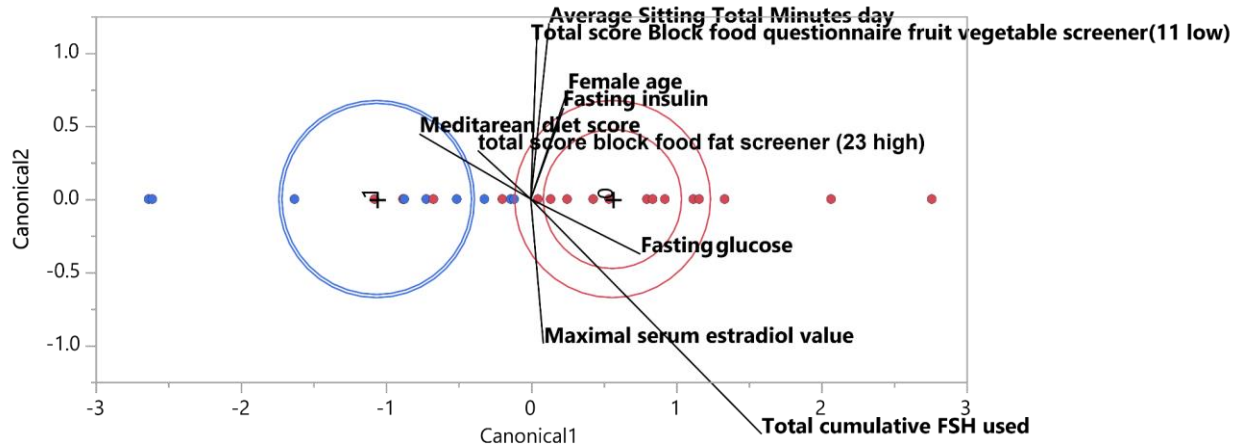


Figure 4: rLDA of 6-weeks of pregnancy and EHR.

- High goodness of separation without misclassification for 6-weeks pregnancy outcomes was achieved with the Metabolite model obtained from Platelet Poor Plasma

In classifying patients into their pregnancy status following IVF, lipids obtained from PPP that did not include the glycerophospholipid (GL) class resulted in one false positive (misclassification = 3.85%, Entropy R-squared = 0.809). Five lipid species were associated with pregnancy failure, those involving CE 17:1 (standardized scoring coefficient = -1.64), CE 22:5 (standardized scoring coefficient = -3.67), FA 20:4 (standardized scoring coefficient = -3.08), capric acid (standardized scoring coefficient = -1.47), and lauric acid (standardized scoring coefficient = -1.72). Successful pregnancies were associated with higher concentrations of CE 18:3 (standardized scoring coefficient = 3.69), CE 20:4 (standardized scoring coefficient = 1.99), CE 20:5 (standardized scoring coefficient = 1.49), FA 20:2 (standardized scoring coefficient = 2.51), arachidic acid (standardized scoring coefficient = 2.26), and myristic acid (standardized scoring coefficient = 2.17).

No change was observed in the percent misclassification (3.85%), nor the number of false positives, when GL species were included as covariates of the lipid model (Entropy R-squared = 0.813). Of note was that circulating total cholesterol (standardized scoring coefficient = 0.350) was positively associated with 6-weeks pregnancy following IVF. Other positively associated covariates included LPE 20:4 (standardized scoring coefficient = 2.60), PC 16:1/18:2 (standardized scoring coefficient = 0.880), PC 17:0/20:3 (standardized scoring coefficient = 1.28), and PI 16:0/18:1 (standardized scoring coefficient = 0.964).

With regards to the metabolite model, none of the patients were misclassified into their pregnancy groups, and relatively high goodness of separation was attained (Entropy R-squared = 0.939). Metabolites, with the exception of 2-ketoisovaleric acid (standardized scoring coefficient = -1.02), glucose-1-phosphate (standardized scoring coefficient = -0.945), and ornithine (standardized scoring coefficient = -1.19), were positively associated with pregnancy and can be viewed in **Figure 5**. These metabolites were 2-hydroxyglutaric acid (standardized scoring coefficient = 1.71), serine (standardized scoring coefficient = 1.15), threonine (standardized scoring coefficient = 1.42), and uric acid (standardized scoring coefficient = 1.47).

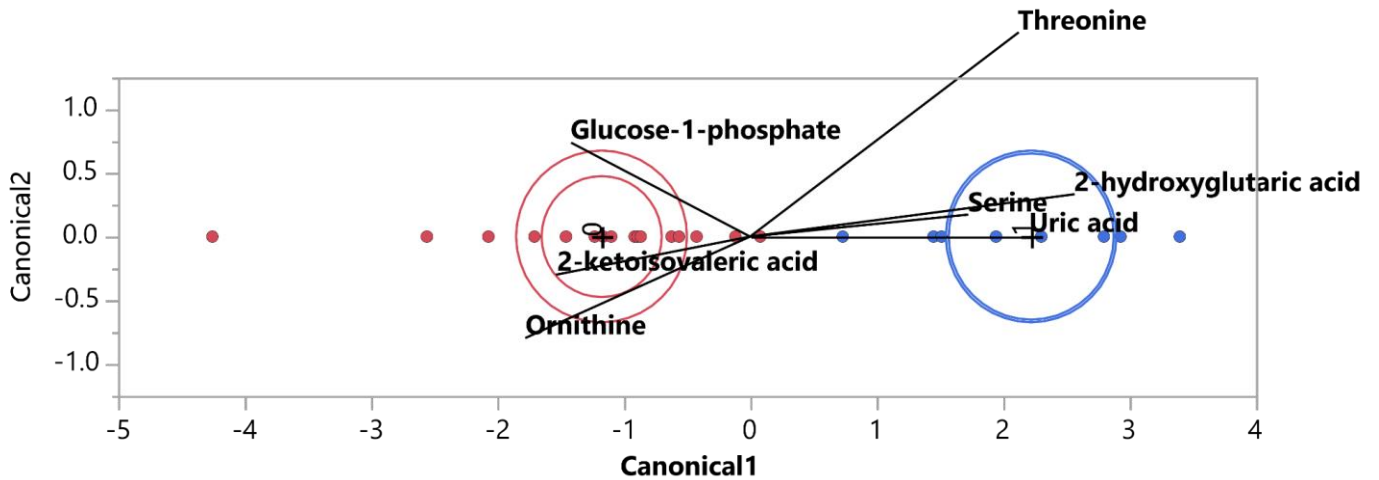


Figure 5: rLDA of 6-weeks of pregnancy and metabolites acquired from PPP.

A final model was constructed without clinical parameters, containing only lipids and metabolites. Total cholesterol (standardized scoring coefficient = 1.30) was positively associated with pregnancy outcomes, as well as LPE 20:4 (standardized scoring coefficient = 1.21), uric acid (standardized scoring coefficient = 1.08), and arachidic acid (standardized scoring coefficient = 0.753). Negatively associated lipids and metabolites, or those that were higher with negative pregnancy outcomes, were LPC 20:4 (standardized scoring coefficient = -1.77), 2-ketoisovaleric acid (standardized scoring coefficient = -0.818), and lauric acid (standardized scoring coefficient = -0.452).

- *Lipids excluding Glycerophospholipids obtained from Follicular Fluid resulted in No Misclassification and the Best Separation for 6-weeks pregnancy groups*

Classification of the 6-week pregnancy groups was achieved with 0% misclassification and high goodness of separation (Entropy R-squared = 0.977) when using a model of lipids, excluding from selection all GL species. Covariates that were weighted heavily

towards pregnancy failure included CE 20:5 (standardized scoring coefficient = -0.959), capric acid (standardized scoring coefficient = -0.870), and stearic acid (standardized scoring coefficient = -1.08). Pregnancy success was associated with higher levels of CE 18:3 (standardized scoring coefficient = 1.31), FA 18:3 (standardized scoring coefficient = 0.867), heptadecanoic acid (standardized scoring coefficient = 1.71), and palmitoleic acid (standardized scoring coefficient = 0.874). Comparatively, this lipid model performed the best against all other FF models for discrimination of the pregnancy classes (**Figure 6**).

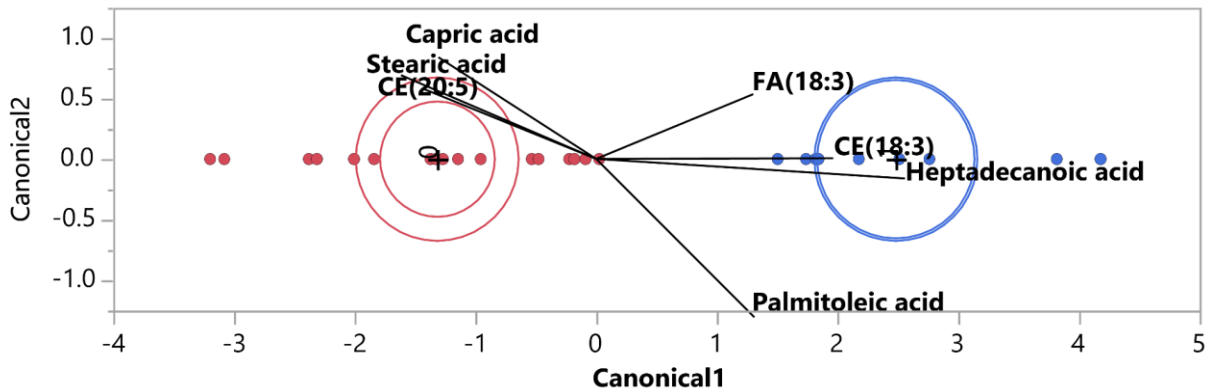


Figure 6: rLDA of 6-weeks of pregnancy and lipids without GL species acquired from FF sample.

Coupling FF obtained lipid species with GL for a model of 6-week pregnancy was achieved with modest misclassification (7.69%) and admissible goodness of separation (Entropy R-squared = 0.750). Lysophospholipids and phospholipids predominated as the covariates of this model where IVF proved efficacious were more closely associated with LPC 14:0 (standardized scoring coefficient = 1.34), LPI 18:1 (standardized scoring coefficient = 0.830), LPI 20:4 (standardized scoring coefficient = 1.47), and PC 18:1/20:3

(standardized scoring coefficient = 1.27). Patients who were classified as having not achieved pregnancy saw higher concentrations of LPC 20:2 (standardized scoring coefficient = -2.07), LPE 18:2 (standardized scoring coefficient = -2.07), and PC 16:0/20:4 (standardized scoring coefficient = -1.06).

Analogous to the 6-week pregnancy lipid model excluding glycerophospholipids, the metabolite model for FF had no misclassification (0%) and high goodness of separation (Entropy R-squared = 0.943). Only alpha-ketoglutarate (standardized scoring coefficient = -1.26) was associated with failed pregnancy. The remaining covariates of fumaric acid (standardized scoring coefficient = 0.793), hexose (standardized scoring coefficient = 0.825), indole-3-propionic acid (standardized scoring coefficient = 0.566), and uric acid (standardized scoring coefficient = 1.35) were associated positively associated with pregnancy.

The final model of FF analytes and clinical parameters for 6-weeks pregnancy status resulted in one false negative (misclassification = 3.85%, Entropy R-squared = 0.889). Despite including all variables across the data domains, only one lipid and metabolites were selected, of which were FA 18:3 (standardized scoring coefficient = 0.616), fumaric acid (standardized scoring coefficient = 1.08), hexose (standardized scoring coefficient = 0.730), and uric acid (standardized scoring coefficient = 1.06) that were positively associated with pregnancy. A singular metabolite, alpha-ketoglutarate (standardized scoring coefficient = -1.29), was elevated in FF for those that did not achieve pregnancy.

Domain Independent and domain-integrated MLRA models predict BMI values with phospholipids and fatty acid derivatives, varied across PPP and FF matrices

Our EHR model for predicting BMI values retrieved fasting glucose, fasting insulin, and the total score from the block food questionnaire fat screener (23 high) as positively associated covariates, while only the average sitting time (total of minutes per day) was negatively associated (R adjusted = 0.769, RMSE = 0.144). Fasting insulin (test statistic = 0.473, Prob > |t| = <0.0001) and total score block food fat screener (23 high; test statistic = 0.167, Prob > |t| = 0.0054) were clinical parameters that were significant after two-way hypothesis testing. As mentioned prior, in constructing the MLRA model, predictors are covaried with another, thus those that were non-significant following the two-way hypothesis test were kept within this clinical parameter model.

- **A multicomponent domain model for PPP outperformed data-domain independent Lipid, Metabolic, and EHR domain models for BMI**

With regards to our PPP PL model, LPC 18:1 (test statistic = -0.261, Prob > |t| = 0.0133), LPC-P 16:0 (test statistic = -0.233, Prob > |t| = 0.0021), PC 16:1/22:6 (test statistic = -0.243, Prob > |t| = 0.0002), and PI 18:0/20:4 (test statistic = -0.268, Prob > |t| = 0.0422) were negatively correlated with an increase in BMI values, while, interestingly, recovered LPC 22:6 (test statistic = 0.305, Prob > |t| = 0.0127) and PC 16:0/22:4 (test statistic = 0.185, Prob > |t| = 0.0027) were positively correlated predictors of BMI values (R adjusted = 0.786, RMSE = 0.138).

From our lipid model excluding PL, lipids that were positively correlated with BMI were CE 18:0 (test statistic = 0.467, Prob > |t| = 0.0014), CE 20:3 (test statistic = 0.364,

Prob > |t| = 0.0015), FA 17:1 (test statistic = 0.691, Prob > |t| = 0.0005), and heptadecanoic acid (test statistic = 0.413, Prob > |t| = 0.0005), while CE 22:4 (test statistic = -0.869, Prob > |t| = <0.0001), FA 14:1 (test statistic = -0.904, Prob > |t| = <0.0001) were negatively correlated (R adjusted = 0.726, RMSE = 0.156).

The metabolic model using PPP metabolites demonstrated that 2-hydroxyglutaric acid (test statistic = -0.203, Prob > |t| = 0.0189), malic acid (test statistic = -0.225, Prob > |t| = 0.0349), serine (test statistic = -0.620, Prob > |t| = <0.0001), and alanine (test statistic = -0.315, Prob > |t| = 0.0144) were negatively correlated with BMI, yet tyrosine (test statistic = 0.276, Prob > |t| = 0.0157), glucose-1-phosphate (test statistic = 0.307, Prob > |t| = 0.0015) were positively correlated (R adjusted = 0.739, RMSE = 0.152).

Inclusion of predictors from all domain models (EHR, PL exclusive, excluding PL, and metabolites) presented the final model with negatively correlated LPC 18:1 (test statistic = -0.210, Prob > |t| = 0.0244), PC 16:1/22:6 (test statistic = -0.090, Prob > |t| = 0.0594), and malic acid (test statistic = -0.207, Prob > |t| = 0.0239) where only PC 16:1/22:6 was not significant following a two-way t-test. Fasting insulin (test statistic = 0.269, Prob > |t| = 0.0018) and PC 16:0/22:4 (test statistic = 0.163, Prob > |t| = 0.0044) were positively correlated with BMI values (R-square adjusted = 0.819, RMSE = 0.127). A visualization of this final model for BMI from EHR data and PPP small molecules can be found in **Figure 7**.

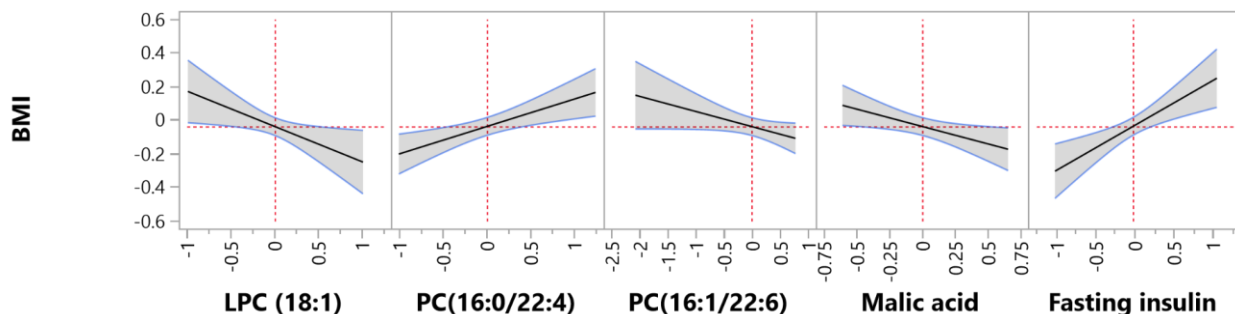


Figure 7: Final model for BMI from EHR data and PPP small molecules.

- Combined data domains for FF enabled the best prediction of BMI values against the other Lipid, Metabolic, and EHR domain models

As determined from FF, the PL model selected fewer lipid species such as LPC 18:2 (test statistic = -0.390, Prob > |t| = 0.0061), and LPC-(11Z-octadeceneyl) (LPC-O) 18:1 (test statistic = -0.466, Prob > |t| = 0.0006) which were negatively correlated with BMI values. Those PL that were positively correlated with BMI included LPC 20:2 (test statistic = 0.385, Prob > |t| = 0.0280), PC 20:3/20:4 (test statistic = 0.193, Prob > |t| = 0.0003) and PE-P 16:0/22:6 (test statistic = 0.478, Prob > |t| = <0.0001). With fewer lipids, the FF PL model achieved a greater fit with a lower RMSE (R adjusted = 0.797, RMSE = 0.134).

From our FF lipid model excluding PL, lipids that positively correlated with BMI involved CE 20:3 (test statistic = 0.855, Prob > |t| = <0.0001), FA 19:0 (test statistic = 0.259, Prob > |t| = 0.0028), and FA 22:2 (test statistic = 0.356, Prob > |t| = 0.0239) while CE 16:0 (test statistic = -0.389, Prob > |t| = 0.0236), CE 18:3 (test statistic = -0.548, Prob > |t| = 0.0004), FA 18:1 (test statistic = -0.648, Prob > |t| = 0.0009) were lipids negatively correlated with BMI (R adjusted = 0.706, RMSE = 0.162).

Few FF metabolites were required to predict BMI values with good fit, those being aspartic acid (test statistic = 0.413, Prob > |t| = 0.0003) and tyrosine (test statistic = 0.583, Prob > |t| = <0.0001) that were positively correlated, and histidine (test statistic = -0.377, Prob > |t| = 0.0285) and indole-3-propionic acid (test statistic = -0.241, Prob > |t| = 0.0008) negatively correlated with BMI (R adjusted = 0.754, RMSE = 0.148).

A combination of all 4 components yielded a final model with PE-P 16:0/22:6 (test statistic = 0.206, Prob > |t| = 0.0040), aspartic acid (test statistic = 0.207, Prob > |t| = 0.0141), and fasting insulin (test statistic = 0.269, Prob > |t| = <0.0001) as positively correlated variables with BMI values, whereas indole-3-propionic acid (test statistic = -0.225, Prob > |t| = <0.0001) was negatively correlated with BMI (R-squared adjusted = 0.856, RMSE = 0.113), the results of which can be viewed in **Figure 8**.

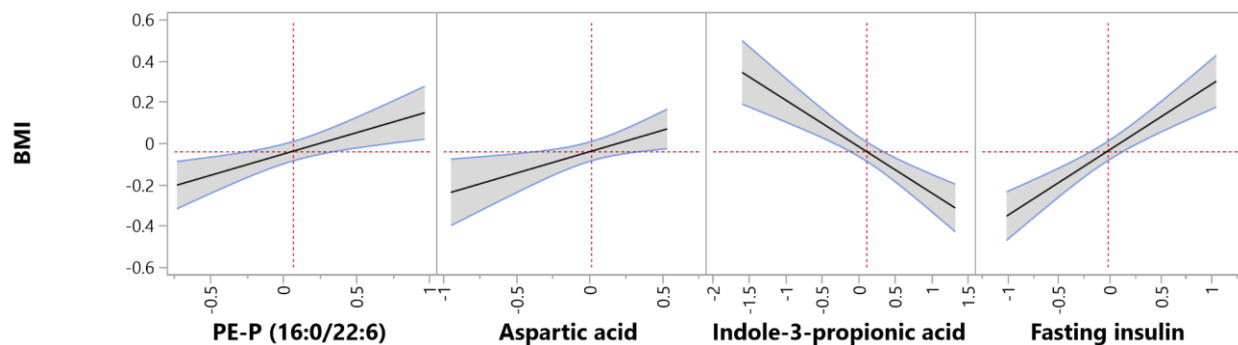


Figure 8: Final model for BMI from EHR data and FF small molecules.

Discussion

This study was able to determine the metabolite and lipid profiles that were specific to changes in body weight, associated with pregnancy outcomes, and correlated to embryo quality following in vitro fertilization (IVF). By measuring two distinct matrices of 26 women, platelet poor plasma (PPP) and follicular fluid (FF), we delineated what matrix interactions were present on the composition of these significant metabolites and lipids and found inter-matrix fluctuations in the levels of these analytes that corresponded with our chosen pregnancy outcomes. Several studies have explored the utility of metabolomics to assess pregnancy outcomes in women of varying weight class

subsequent IVF, yet were restrained in their findings by the level of specificity in their analyses or by not considering matrix effects⁹⁴⁻⁹⁷.

Maternal central carbon metabolism undergoes substantial alterations early in gestation. One such example includes 2-hydroxyglutaric acid (2-HG), a derivative of Krebs cycle intermediate 2-oxoglutarate that, when obtained from PPP, was positively associated with pregnancy. Respiratory alkalosis is a common acid-base disorder that is observed in pregnancies, and the L-enantiomer of 2-HG accumulates in the context of a hypoxic ventilatory response to alleviate reductive stress¹⁰⁸⁻¹¹². With regards to pregnancy, the metabolic pathway of L-2-HG in humans is poorly characterized and requires further study. Carbohydrates and lipid metabolites have also served as putative markers of embryo quality^{97,113,114}. Glucose-1-phosphate (G-1-P) obtained from PPP (Figure 5), at high concentrations, was negatively associated with pregnancy; notably, pregnancy alters glucose-6-phosphate dehydrogenase activity resulting in enzymatic deficiency¹¹⁵. Furthermore, plasma concentrations of glycogen phosphorylase, which catalyzes the rate-limiting step of glycogen to G-1-P, are elevated in pregnant women experiencing preterm preeclampsia¹¹⁶. We found that in PPP, the higher the concentration of phosphate, the greater 2PN values. Phosphate serves as an intracellular buffer and regulates the death of hypertrophic cells via caspase-9-mediated pathways¹¹⁷. Mechanistic studies on oocyte progression to the blastocyst stage however have demonstrated that media devoid of glucose and phosphate, but enriched in glutamine, improves the development of embryos^{118,119}, complicating the interaction between phosphate and oocyte maturation.

Amino acid metabolism is also altered throughout the course of pregnancy; relative to the first trimester, 2-ketoisovaleric acid, a keto-acid (BCKA) intermediate within branched-chain amino acid catabolism (BCAA), has been shown to decrease in plasma^{112,120}. Elevated 2-ketoisovaleric acid (KV) is indicative of impaired BCAA, where an accumulation of toxic BCKA can promote the development of type 2 diabetes mellitus¹²⁰. Our results confirm the deleterious effects of accumulated BCKA like KV, when obtained from PPP, as higher KV was correlated with lower 2PN values and was negatively associated with clinical pregnancies. From our study, plasma concentrations of 3-aminoisobutyric acid (BAIBA) and glutamic acid decreased with 2PN values. Degradation of BAIBA, an endogenous protective myokine, regulates adipose tissue browning and improves insulin sensitivity¹²¹. A reduction in the turnover rate, or a higher concentration, of amino acids like glutamic acid track with meiotic phase progression. An increase in glutamic acid corresponds with oocyte degradation¹²². Pregnancy is a period of extreme physiological demand for protein synthesis. The anionic form of glutamic acid, glutamate, plays a vital role in protein synthesis and persists at low concentrations throughout gestation so that proteins may be retained to meet the metabolic demand; hence, elevated glutamic acid may indicate a breakdown in protein synthesis¹²³. Obtained from PPP, ornithine was elevated in response to higher 2PN values (Figure 2), however curiously higher ornithine concentrations corresponded with unsuccessful pregnancy following IVF. Ornithine can act as a substrate for putrescine synthesis, a conjugate base that positively influences oocyte maturation; however, elevation of ornithine may also correspond with an inborn error in the urea cycle^{124,125}. Future studies that parse out the exact role plasma ornithine has towards pregnancy outcomes.

When eliciting the effect of fatty acids (FA), it is of great import to determine where particular FAs are sequestered within the lipidome. Our analysis revealed free fatty acid and glycerophospholipid species consisting of capric acid (FA 10:0), palmitic acid (FA 16:0), palmitoleic acid (FA 16:1), heptadecanoic acid (FA 17:0), stearic acid (FA 18:0), oleic acid (FA 18:1), linoleic acid (FA 18:2), α -linoleic acid (FA 18:3), arachidonic acid (FA 20:4), docosatetraenoic acid (FA 22:4), and docosahexaenoic acid (FA 22:6) to elicit differential effects on embryo quality, body mass composition, and clinical pregnancy outcomes, dependent upon matrix. Accumulation of nonesterified FA 10:0 and FA 18:0 in FF was found to be negatively associated with 6-weeks clinical pregnancy, while greater concentrations of FA 17:0 and FA 18:3 were positively associated with achieving clinical pregnancy post IVF. Capric acid (FA 10:0) regulates inflammation by functioning as a modulating ligand for peroxisome proliferator-activated receptors, and by interfering with nuclear factor kappa beta activation^{126,127}. Stearic acid (FA 18:0) along with palmitic acid (FA 16:0), which are the predominant saturated free fatty acids in FF¹²⁸, activate inflammatory signaling pathways and can induce endoplasmic reticulum stress^{129,130}. Previous studies found that embryos which released greater concentrations of FA 10:0 and FA 18:0 into the microenvironment emulsion saw a greater reduction in birth¹³¹. Conversely, FA 18:3, an essential ω -3 polyunsaturated FA, is evinced to increase the number of mature oocytes in a dose-dependent fashion¹³². Additionally, high concentrations of cholesteryl esters (CE) bearing FA 18:3 (CE 18:3) were positively associated with pregnancy, while CE 20:5 higher concentrations in FF were negatively associated with pregnancy. Cholesteryl esters can accumulate in steroidogenic cells as

well as in pools of lipid droplets; their main functions are to store and transport cholesterol as well as PUFA¹³³. These PUFA are then integrated into steroidogenesis, and can serve as precursors to prostanoids and lipoxygenase products as well as signaling molecules¹³⁴.

The number of two polar bodies (2PN) increased with higher concentrations of LPI 18:1, LPE 20:4, LPC 22:4 in FF, whereas LPC 16:1 and LPI 18:2 were negatively correlated with 2PN. Interestingly, absolute plasma concentrations of LPI 18:2 among other lysophospholipids (lysoPL) are significantly reduced with gestational diabetes mellitus (GDM), possibly due to an altered glucose metabolism; additionally, the ratio of saturated lysoPL - to - unsaturated lysoPL is higher during pregnancy with GDM, indicating that lysoPL acyl moieties may determine the effect of lysoPL species in lipid metabolic pathways¹³⁵. Platelet poor plasma LPC 18:1, a purported inhibitor of reactive oxygen species synthesis and neutrophil effector responses, was found here to negatively correlate with BMI values¹³⁶. Species such as LPC 20:4 and LPC 22:4 can potentiate anti-inflammatory effects, neutralizing LPCs that have been shown to transduce pro-inflammatory signals such as LPC 16:0, and these very species are known to be altered significantly in the serum of obese women^{137,138}. Lysophospholipids therefore may serve as markers of oxidative stress, lipotoxicity, and other inflammatory factors that regulate embryo quality and body composition^{109,138,139}. Yet the physiological role of lysophospholipids, especially by their native matrix, are nascently understood despite their apparent involvement in numerous inflammatory, proliferative, and cytoskeletal responses as signaling molecules¹³⁸.

Stereoisomeric and structural, or “positional”, isomeric lipids can have markedly different biological ramifications for overall health and pregnancy outcomes. The position of a fatty acyl moiety affects its distribution in phospholipid species. Phosphatidylcholines (PC) such as PC 16:0/22:4 acquired from PPP, and PC 16:0/22:6 obtained from FF, were positively correlated with rising BMI values, while PC 16:1/22:6 was negatively correlated with BMI. Interestingly, PCs containing FA 22:6, an ω -3 polyunsaturated fatty acid that serves as a precursor for several pro-resolving lipid mediators¹⁴⁰, varied here in its association with BMI dependent upon other fatty acyl chains in the *sn*1 position. While FA 22:6 has also been linked to positively influence biochemical processes in fetal development^{141,142}, these data exemplify the importance of metabolomic analyses to characterize the lipidome with a greater level of specificity that can capture the physicochemical properties of lipids.

Palmitic acid is a saturated FA that at high concentrations induces a proinflammatory response, as determined by cytokine and adipokine profiling; furthermore, elevated nonesterified palmitate correlates with insulin resistance in pregnant women¹²⁹ and at higher plasma concentrations is associated with a reduction in the number of births¹³¹. Reesterification of LPC to PC, and de novo synthesis of PC species such as PC 16:0/22:4, have been found to be amplified by the metabolic dysregulations typical of an obese state¹⁴³. The inverse is true for palmitoleic acid (FA 16:1) bearing PCs; additionally, we found nonesterified FA 16:1, when obtained from FF,

at higher concentrations to be positively associated with clinical pregnancy, 6 weeks subsequent IVF. Palmitoleic acid is a lipokine that exhibits insulin-sensitizing and anti-inflammatory properties. During maternal obesity, it has been reported that the synthesis of free form palmitoleic acid, and storage lipids bearing FA 16:1, is downregulated¹⁴¹. Two plasmalogens obtained from FF also correlated with pregnancy outcomes, with an ethanolamine plasmalogen (PE-P 16:0/22:6) positively correlating with BMI, and a choline plasmalogen (PC-P 18:0/22:6) negatively correlating with 2PN values. Concentrations of these lipid species tend to fluctuate with the physiological processes such as aging and serve as putative biomarkers of ovarian reserve when assayed from FF¹⁴⁴. Although the functions of plasmalogens are not fully understood, the literature suggests that these lipids act as reservoirs of PUFA, such as FA 22:6, to be further metabolized into second messenger molecules involved in regulating inflammation^{144,145}.

Acylcarnitine species esterified to palmitate for example (acylcarnitine FA 16:0), when obtained from FF, increases with 2PN values. It has previously been reported that IVF may result in excess carnitine consumption and greater depletion of long-chain acylcarnitine pools by oocytes¹⁴⁶. Ergo, a positive correlation for acylcarnitine C16:0 and 2PN values may suggest metabolic processes, such as a complete tricarboxylic acid cycle, that follow the course of pregnancy. Additionally, oleic acid (FA 18:1) bearing acylcarnitines, when obtained from FF, decreased with 2PN values. Oocyte competence can be negatively impacted by saturated free fatty acids like stearic acid and palmitic acid. When not sequestered to β -oxidation, free form oleic acid and palmitoleic acid can stimulate the distribution of saturated FA towards neutral storage lipids and β -oxidation, away from apoptotic, pro-inflammatory pathways^{141(p),147,148}.

Uric acid was positively associated with clinical pregnancy, when it was obtained from PPP. Early pregnancy serum uric acid levels tend to fall, related to the uricosuric effects from estrogen. Uric acid is also positively associated with insulin resistance, hence this finding elicits further study as to determine why uric acid was positively associated with pregnancy. In general, uric acid concentration decreases during the first three months of normal pregnancy due to increased glomerular filtration rate (GFR). However, a previous study showed that the concentration of uric acid in the plasma of women undergoing IVF decreased less than the women who had a normal pregnancy¹⁴⁹. To our knowledge, there are limited studies that assess kidney function and GFR in IVF. Another possible explanation for our finding of uric acid increasing with pregnancy is that IVF may increase the chance of induction of preeclampsia¹⁵⁰. Conceptions achieved by IVF resulted in a greater risk to develop preeclampsia (2.7 times)^{151,152}.

Indole-3-propionic acid (IPA), synthesized from tryptophan and a natural product derived from the gut microbiota, has been associated with insulin secretion and sensitivity, and negatively correlated with low-grade inflammation. This could be due to IPA being the most potent scavenger of the hydroxyl radicals, and elevated concentrations of IPA in plasma is associated with reduced risk for incident type 2 diabetes (T2D); yet this protective effect may be diminished or negated in patients who already have T2D. Obesity has had a documented signature on the metabolomic profile of FF, decreases IPA in FF as we determined here with higher BMI values. These data suggest that IPA obtained from FF may model antioxidant status, or a reflect the gut metabolism interacting with follicular development¹⁵³. IPA can also reduce the levels of various lipid peroxidation markers and DNA damage. In a previous study using rats

model, IPA was shown to improve the serum insulin resistance index, glucose, and insulin levels. Obesity has been studied in animals and humans. It causes alteration of bacterial species in the gut microbiome compared to controls. Considering this, Ruebel et al. hypothesized that obesity changes the profiles of bacteria species, reducing IPA production. Alternatively, the systemic inflammation caused by obesity could cause intestinal inflammation, which would modulate the gut microbiome and lower IPA levels. Future research in germ-free models will be needed to confirm this hypothesis as well as determine the role of FF IPA in oocyte maturation and development¹⁵³.

Malic acid from PPP is exogenous, obtained from a diet of citric fruits, and was also found to be negatively associated with BMI values (figure 7). Dietary choices and cooking methods may explain the decline for the obese group. The natural sources of malic acid ($p = 0.026$) are typically vegetables, berries, cherries, and citrus fruits; more recently, it has been incorporated into popular fruit vinegar drinks for its antioxidant properties and taste, suggesting that higher malic acid in PPP could result in a patient with lower systemic oxidative stress⁶ (Figure 6). As the relation between obesity and oxidative stress is well characterized in previous research^{154,155}, an in vitro study shows that the decrease in malic acid concentration is an oxidative stress biomarker besides vitamin C¹⁵⁶.

Beta-alanine is a nonessential amino acid that was negatively associated with 2PN values as obtained from PPP (figure 2). During pregnancy, the development of gluconeogenesis is attenuated due to decreased alanine flux. This process is triggered by the intrahepatic mechanism which lowers the deamination of alanine¹⁵⁷. It has been hypothesized that the metabolic cooperation between oocytes and follicular cells leads to

the uptake of amino acids. In addition, these findings indicate that the cells do not have the capability to increase the level of leucine in mice. A liquid chromatography-tandem Mass spectrometry study revealed that the presence of aromatic amino acids in the fluid of polycystic ovary syndrome (PCOS) patients is associated with an increase in body mass index. These changes involve elevation of amino acids including glutamic acid, phenylalanine, alanine, and arginine. The study supports the notion that the lack of these nutrients can affect the quality of oocyte eggs. A previous study showed that evaluation of the non-invasive amino acid profiling of bovine oocytes with high-performance LC might be utilized to evaluate oocyte development in bovine. The results showed a significant decrease in glutamine and increase in alanine in the medium of oocytes that failed in the cleavage process after 3 days postfertilization¹²².

Aspartic acid is interestingly correlated with higher BMI values as well as a greater number of 2PN. A previous study showed that increased aspartic acid in PCOS women is related to increased chance of getting pregnant¹⁵⁸. In addition, D'Aniello et al. demonstrate a positive relation between aspartic acid elevation and egg quality in obese women undergoing IFV¹⁵⁹. Furthermore, d-aspartic acid improves the synthesis of some hormones such as LH and testosterone¹⁶⁰. The LH hormone released from the anterior pituitary gland is essential for pregnancy sustained through activation of corpus luteum which in turn causes production of progesterone¹⁶¹. The mid-cycle luteinization surge is known to play a crucial role in the development of the oocyte and the follicularization process. However, recent studies indicate that the abnormal level of LH may be detrimental to the embryo development. In addition, the reduction in concentrations of human LH in the follicular fluid can cause decreased production of follicle-stimulating

hormones (FSH). This study supports the hypothesis that decreased concentrations of LH can affect the quality of oocytes¹⁵⁹.

Serine was positively associated with pregnancy along with threonine in platelet poor plasma. Valine, glycine, serine, and threonine concentrations in plasma were closely correlated with insulin resistance and obesity. In addition, a significant positive association of lactate and leucine concentrations with insulin resistance was observed regardless of obesity. Notably, significant decreases in serine and threonine concentration were observed in obese women with PCOS and patients with insulin resistance compared to non-obese PCOS patients and patients with normal insulin sensitivity, suggesting opposing effects of PCOS and their two common features on serine and threonine metabolism¹⁶². An earlier study on obese mice supplemented with threonine for 10 weeks showed weight reduction and improvement of insulin resistance¹⁶³. In addition, a cross-sectional study evaluating the association of amino acids regarding insulin sensitivity in men showed a significant association between serine concentration and insulin sensitivity improvement¹⁶⁴.

In summation, our findings here of lipid species being correlated with 2PN values provides a basis for the detrimental effects of high BMI, and the lipid disruptions that accompany this physical state, on embryo quality and success of clinical pregnancy. Group II ovulatory disorders compose ~85% of all ovulation disorders and are caused by conditions such as abnormal BMI. Obesity is known to result in disruptions to endocrine and paracrine mechanisms such as insulin signaling, which is evinced to act on the HPO axis and can lead to adverse pregnancy outcomes.

Limitations with this analysis included a small cohort size, which carried the risk of overfitting our regression estimates. Standardization of the regression coefficients aided us in overcoming this challenge, and reliance on adjusted R-squared as a performance metric meant that our measures were adjusted to produce unbiased estimators of the population and effect. Relative quantification¹⁶⁵ of circulating lipids and metabolites enabled us to determine the specific species that were correlated with the number of distinct pronuclei and two polar bodies (2PN) or embryo quality, molecules correlated with BMI, and putative markers for successful pregnancies following IVF.

Bibliography

1. Daak AA, Ghebremeskel K, Mariniello K, Attallah B, Clough P, Elbashir MI. Docosahexaenoic and eicosapentaenoic acid supplementation does not exacerbate oxidative stress or intravascular haemolysis in homozygous sickle cell patients. *Prostaglandins, Leukotrienes and Essential Fatty Acids*. 2013;89(5):305-311. doi:10.1016/j.plefa.2013.09.006
2. Davis H, Gergen PJ, Moore RM. Geographic differences in mortality of young children with sickle cell disease in the United States. *Public Health Rep*. 1997;112(1):52-58.
3. Sundd P, Gladwin MT, Novelli EM. Pathophysiology of Sickle Cell Disease. *Annu Rev Pathol*. 2019;14:263-292. doi:10.1146/annurev-pathmechdis-012418-012838
4. Saraf SL, Molokie RE, Nourai M, et al. Differences in the clinical and genotypic presentation of sickle cell disease around the world. *Paediatr Respir Rev*. 2014;15(1):4-12. doi:10.1016/j.prrv.2013.11.003
5. Han X. Lipidomics for precision medicine and metabolism: A personal view. *Biochimica et Biophysica Acta (BBA) - Molecular and Cell Biology of Lipids*. 2017;1862(8):804-807. doi:10.1016/j.bbalip.2017.02.012
6. Stephenson DJ, Hoferlin LA, Chalfant CE. Lipidomics in translational research and the clinical significance of lipid-based biomarkers. *Transl Res*. 2017;189:13-29. doi:10.1016/j.trsl.2017.06.006
7. Nur E, Biemond BJ, Otten HM, Brandjes DP, Schnog JJB. Oxidative stress in sickle cell disease; pathophysiology and potential implications for disease management. *American Journal of Hematology*. 2011;86(6):484-489. doi:10.1002/ajh.22012

8. Cordovil K. Sickle Cell Disease: A Genetic Disorder of Beta-Globin. *Thalassemia and Other Hemolytic Anemias*. Published online July 11, 2018. doi:10.5772/intechopen.74778
9. Inusa BPD, Hsu LL, Kohli N, et al. Sickle Cell Disease—Genetics, Pathophysiology, Clinical Presentation and Treatment. *International Journal of Neonatal Screening*. 2019;5(2):20. doi:10.3390/ijns5020020
10. Manwani D, Frenette PS. Vaso-occlusion in sickle cell disease: pathophysiology and novel targeted therapies. *Blood*. 2013;122(24):3892-3898. doi:10.1182/blood-2013-05-498311
11. Bender MA. Sickle Cell Disease. In: Adam MP, Ardinger HH, Pagon RA, et al., eds. *GeneReviews®*. University of Washington, Seattle; 1993. Accessed March 10, 2020. <http://www.ncbi.nlm.nih.gov/books/NBK1377/>
12. Grosse SD, Odame I, Atrash HK, Amendah DD, Piel FB, Williams TN. Sickle Cell Disease in Africa. *Am J Prev Med*. 2011;41(6):S398-S405. doi:10.1016/j.amepre.2011.09.013
13. Mburu J, Odame I. Sickle cell disease: Reducing the global disease burden. *International Journal of Laboratory Hematology*. 2019;41(S1):82-88. doi:10.1111/ijlh.13023
14. Aygun B, Odame I. A global perspective on sickle cell disease. *Pediatric Blood & Cancer*. 2012;59(2):386-390. doi:10.1002/pbc.24175
15. Piel FB, Hay SI, Gupta S, Weatherall DJ, Williams TN. Global burden of sickle cell anaemia in children under five, 2010-2050: modelling based on demographics, excess mortality, and interventions. *PLoS Med*. 2013;10(7):e1001484. doi:10.1371/journal.pmed.1001484

16. AlHamdan NA, AlMazrou YY, AlSwaidi FM, Choudhry AJ. Premarital screening for thalassemia and sickle cell disease in Saudi Arabia. *Genetics in Medicine*. 2007;9(6):372-377. doi:10.1097/GIM.0b013e318065a9e8
17. Jastaniah W. Epidemiology of sickle cell disease in Saudi Arabia. *Ann Saudi Med*. 2011;31(3):289-293. doi:10.4103/0256-4947.81540
18. Ojodu J, Hulihan MM, Pope SN, Grant AM. Incidence of Sickle Cell Trait — United States, 2010. *MMWR Morb Mortal Wkly Rep*. 2014;63(49):1155-1158.
19. Piel FB, Steinberg MH, Rees DC. Sickle Cell Disease. *New England Journal of Medicine*. 2017;376(16):1561-1573. doi:10.1056/NEJMra1510865
20. Steiner CA, Miller JL. Sickle Cell Disease Patients in U.S. Hospitals, 2004: Statistical Brief #21. In: *Healthcare Cost and Utilization Project (HCUP) Statistical Briefs*. Agency for Healthcare Research and Quality (US); 2006. Accessed July 9, 2020. <http://www.ncbi.nlm.nih.gov/books/NBK63489/>
21. Du S, Lin C, Tao YX. Updated mechanisms underlying sickle cell disease-associated pain. *Neuroscience Letters*. 2019;712:134471. doi:10.1016/j.neulet.2019.134471
22. Steinberg MH, Sebastiani P. Genetic Modifiers of Sickle Cell Disease. *Am J Hematol*. 2012;87(8):795-803. doi:10.1002/ajh.23232
23. Aich A, Beitz AJ, Gupta K. Mechanisms of Pain in Sickle Cell Disease. *Sickle Cell Disease - Pain and Common Chronic Complications*. Published online November 10, 2016. doi:10.5772/64647
24. Ballas SK. Current Issues in Sickle Cell Pain and Its Management. *Hematology Am Soc Hematol Educ Program*. 2007;2007(1):97-105. doi:10.1182/asheducation-2007.1.97

25. Khasabova IA, Uhelski M, Khasabov SG, Gupta K, Seybold VS, Simone DA. Sensitization of nociceptors by prostaglandin E₂-glycerol contributes to hyperalgesia in mice with sickle cell disease. *Blood*. 2019;133(18):1989-1998. doi:10.1182/blood-2018-11-884346
26. van Tits LJ, van Heerde WL, Landburg PP, et al. Plasma annexin A5 and microparticle phosphatidylserine levels are elevated in sickle cell disease and increase further during painful crisis. *Biochemical and Biophysical Research Communications*. 2009;390(1):161-164. doi:10.1016/j.bbrc.2009.09.102
27. Ambrogini P, Torquato P, Bartolini D, et al. Excitotoxicity, neuroinflammation and oxidant stress as molecular bases of epileptogenesis and epilepsy-derived neurodegeneration: The role of vitamin E. *Biochimica et Biophysica Acta (BBA) - Molecular Basis of Disease*. 2019;1865(6):1098-1112. doi:10.1016/j.bbadis.2019.01.026
28. Connor WE, Lin DS, Thomas G, Ey F, DeLoughery T, Zhu N. Abnormal phospholipid molecular species of erythrocytes in sickle cell anemia. *J Lipid Res*. 1997;38(12):2516-2528.
29. Daak AA, Ghebremeskel K, Hassan Z, et al. Effect of omega-3 (n-3) fatty acid supplementation in patients with sickle cell anemia: randomized, double-blind, placebo-controlled trial. *Am J Clin Nutr*. 2013;97(1):37-44. doi:10.3945/ajcn.112.036319
30. Setty BN, Chen D, Stuart MJ. Sickle cell vaso-occlusive crisis is associated with abnormalities in the ratio of vasoconstrictor to vasodilator prostanoids. *Pediatr Res*. 1995;38(1):95-102. doi:10.1203/00006450-199507000-00017
31. Gupta M, Msambichaka L, Ballas SK, Gupta K. Morphine for the Treatment of Pain in Sickle Cell Disease. *The Scientific World Journal*. doi:https://doi.org/10.1155/2015/540154

32. Trang T, Quirion R, Jhamandas K. The spinal basis of opioid tolerance and physical dependence: Involvement of calcitonin gene-related peptide, substance P, and arachidonic acid-derived metabolites. *Peptides*. 2005;26(8):1346-1355.
doi:10.1016/j.peptides.2005.03.031
33. Laino CH. Innovations in Pain Management: Morphine Combined with Omega-3 Fatty Acids. *The Open Conference Proceedings Journal*. 2017;8(1).
doi:10.2174/221028901708010052
34. Escudero GE, Romañuk CB, Toledo ME, Olivera ME, Manzo RH, Laino CH. Analgesia enhancement and prevention of tolerance to morphine: beneficial effects of combined therapy with omega-3 fatty acids. *Journal of Pharmacy and Pharmacology*. 2015;67(9):1251-1262. doi:10.1111/jphp.12416
35. Matte A, Recchiuti A, Federti E, et al. Resolution of sickle cell disease-associated inflammation and tissue damage with 17R-resolvin D1. *Blood*. 2019;133(3):252-265.
doi:10.1182/blood-2018-07-865378
36. Ahn K, Johnson DS, Cravatt BF. Fatty acid amide hydrolase as a potential therapeutic target for the treatment of pain and CNS disorders. *Expert Opin Drug Discov*. 2009;4(7):763-784. doi:10.1517/17460440903018857
37. Uhelski ML, Gupta K, Simone DA. Sensitization of C-fiber nociceptors in mice with sickle cell disease is decreased by local inhibition of anandamide hydrolysis. *Pain*. 2017;158(9):1711-1722. doi:10.1097/j.pain.0000000000000966
38. Lang F, Qadri SM. Mechanisms and Significance of Eryptosis, the Suicidal Death of Erythrocytes. *BPU*. 2012;33(1-3):125-130. doi:10.1159/000334163

39. Repsold L, Joubert AM. Eryptosis: An Erythrocyte's Suicidal Type of Cell Death. *BioMed Research International*. doi:<https://doi.org/10.1155/2018/9405617>
40. Farooq S, Abu Omar M, Salzman GA. Acute chest syndrome in sickle cell disease. *Hospital Practice*. 2018;46(3):144-151. doi:10.1080/21548331.2018.1464363
41. Klings ES, Christman BW, McCLUNG J, et al. Increased F2 Isoprostanes in the Acute Chest Syndrome of Sickle Cell Disease as a Marker of Oxidative Stress. *Am J Respir Crit Care Med*. 2001;164(7):1248-1252. doi:10.1164/ajrccm.164.7.2101020
42. Gladwin MT. Pulmonary Complications of Sickle Cell Disease. *n engl j med*. Published online 2008:12.
43. Jain S, Bakshi N, Krishnamurti L. Acute Chest Syndrome in Children with Sickle Cell Disease. *Pediatr Allergy Immunol Pulmonol*. 2017;30(4):191-201. doi:10.1089/ped.2017.0814
44. Vichinsky EP, Neumayr LD, Earles AN, et al. Causes and Outcomes of the Acute Chest Syndrome in Sickle Cell Disease. *New England Journal of Medicine*. 2000;342(25):1855-1865. doi:10.1056/NEJM200006223422502
45. Styles L, Schalkwijk C, Aarsman A, Vichinsky E, Lubin B, Kuypers F. Phospholipase A2 levels in acute chest syndrome of sickle cell disease. *Blood*. 1996;87(6):2573-2578. doi:10.1182/blood.V87.6.2573.bloodjournal8762573
46. Ren H, Ghebremeskel K, Okpala I, Ugochukwu CC, Crawford M, Ibegbulam O. Abnormality of erythrocyte membrane n-3 long chain polyunsaturated fatty acids in sickle cell haemoglobin C (HbSC) disease is not as remarkable as in sickle cell anaemia (HbSS).

Prostaglandins, Leukotrienes and Essential Fatty Acids. 2006;74(1):1-6.

doi:10.1016/j.plefa.2005.10.002

47. Patel SR, Zimring JC. Transfusion Induced Bone Marrow Transplant Rejection Due to Minor Histocompatibility Antigens. *Transfus Med Rev*. 2013;27(4):241-248.
doi:10.1016/j.tmr.2013.08.002
48. Ataga KI, Moore CG, Hillery CA, et al. Coagulation activation and inflammation in sickle cell disease-associated pulmonary hypertension. *Haematologica*. 2008;93(1):20-26.
doi:10.3324/haematol.11763
49. Buseri FI, Shokunbi WA, Jeremiah ZA. Plasma fibrinogen levels in Nigerian homozygous (Hb SS) sickle cell patients. *Hemoglobin*. 2007;31(1):89-92.
doi:10.1080/03630260601059217
50. Tomer A, Harker LA, Kasey S, Eckman JR. Thrombogenesis in sickle cell disease. *The Journal of Laboratory and Clinical Medicine*. 2001;137(6):398-407.
doi:10.1067/mlc.2001.115450
51. Zimmerman GA, McIntyre TM, Prescott SM, Stafforini DM. The platelet-activating factor signaling system and its regulators in syndromes of inflammation and thrombosis. *Critical Care Medicine*. 2002;30(5):S294.
52. Oh SO, Ibe BO, Johnson C, Kurantsin-mills J, Raj JU. Platelet-activating factor in plasma of patients with sickle cell disease in steady state. *Journal of Laboratory and Clinical Medicine*. 1997;130(2):191-196. doi:10.1016/S0022-2143(97)90095-0

53. Mariano F, Bussolati B, Migliori M, Russo S, Triolo G, Camussi G. Platelet-Activating Factor Synthesis by Neutrophils, Monocytes, and Endothelial Cells is Modulated by Nitric Oxide Production. *Shock*. 2003;19(4):339-344.
54. Villagra J, Shiva S, Hunter LA, Machado RF, Gladwin MT, Kato GJ. Platelet activation in patients with sickle disease, hemolysis-associated pulmonary hypertension, and nitric oxide scavenging by cell-free hemoglobin. *Blood*. 2007;110(6):2166-2172.
doi:10.1182/blood-2006-12-061697
55. Mack AK, Kato GJ. Sickle cell disease and nitric oxide: A paradigm shift? *Int J Biochem Cell Biol*. 2006;38(8):1237-1243. doi:10.1016/j.biocel.2006.01.010
56. Wun T. The Role of Inflammation and Leukocytes in the Pathogenesis of Sickle Cell Disease. *Hematology*. 2000;5(5):403-412. doi:10.1080/10245332.2000.11746536
57. Haynes J, Obiako B. Activated polymorphonuclear cells increase sickle red blood cell retention in lung: role of phospholipids. *Am J Physiol Heart Circ Physiol*. 2002;282(1):H122-130. doi:10.1152/ajpheart.2002.282.1.H122
58. Setty BNY, Kulkarni S, Stuart MJ. Role of erythrocyte phosphatidylserine in sickle red cell-endothelial adhesion. *Blood*. 2002;99(5):1564-1571. doi:10.1182/blood.V99.5.1564
59. Sparkenbaugh E, Pawlinski R. Interplay between coagulation and vascular inflammation in sickle cell disease. *Br J Haematol*. 2013;162(1). doi:10.1111/bjh.12336
60. Hargens AR, Bowie LJ, Lent D, et al. Sickle-cell hemoglobin: fall in osmotic pressure upon deoxygenation. *Proc Natl Acad Sci U S A*. 1980;77(7):4310-4312.
61. Lang PA. Stimulation of erythrocyte ceramide formation by platelet-activating factor. *Journal of Cell Science*. 2005;118(6):1233-1243. doi:10.1242/jcs.01730

62. Miller ML, Gao G, Pestina T, Persons D, Tuomanen E. Hypersusceptibility to Invasive Pneumococcal Infection in Experimental Sickle Cell Disease Involves Platelet-Activating Factor Receptor. *J Infect Dis.* 2007;195(4):581-584. doi:10.1086/510626
63. McGann PT, Ware RE. Hydroxyurea therapy for sickle cell anemia. *Expert Opin Drug Saf.* 2015;14(11):1749-1758. doi:10.1517/14740338.2015.1088827
64. Okam MM, Shaykevich S, Ebert BL, Zaslavsky AM, Ayanian JZ. National Trends in Hospitalizations for Sickle Cell Disease in the United States following the FDA Approval of Hydroxyurea, 1998 to 2008. *Med Care.* 2014;52(7):612-618. doi:10.1097/MLR.0000000000000143
65. Cieri-Hutcherson NE, Hutcherson TC, Conway-Habes EE, Burns BN, White NA. Systematic Review of L-glutamine for Prevention of Vaso-occlusive Pain Crisis in Patients with Sickle Cell Disease. *Pharmacotherapy: The Journal of Human Pharmacology and Drug Therapy.* 2019;39(11):1095-1104. doi:10.1002/phar.2329
66. Agrawal RK, Patel RK, shah V, Nainiwal L, Trivedi B. Hydroxyurea in Sickle Cell Disease: Drug Review. *Indian J Hematol Blood Transfus.* 2014;30(2):91-96. doi:10.1007/s12288-013-0261-4
67. Baliga BS, Pace BS, Chen HH, Shah AK, Yang YM. Mechanism for fetal hemoglobin induction by hydroxyurea in sickle cell erythroid progenitors. *American Journal of Hematology.* 2000;65(3):227-233. doi:10.1002/1096-8652(200011)65:3<227::AID-AJH9>3.0.CO;2-V
68. Lanzkron S, Strouse JJ, Wilson R, et al. Systematic Review: Hydroxyurea for the Treatment of Adults with Sickle Cell Disease. *Annals of Internal Medicine.* 2008;148(12):939-955. doi:10.7326/0003-4819-148-12-200806170-00221

69. Quinn CT. I-Glutamine for sickle cell anemia: more questions than answers. *Blood*. 2018;132(7):689-693. doi:10.1182/blood-2018-03-834440
70. Bolaños-Meade J, Brodsky RA. Blood and marrow transplantation for sickle cell disease: Is less more? *Blood Reviews*. 2014;28(6):243-248. doi:10.1016/j.blre.2014.08.001
71. Hoppe CC, Walters MC. Bone marrow transplantation in sickle cell anemia. *Current Opinion in Oncology*. 2001;13(2):85-90.
72. Bhatia M, Walters MC. Hematopoietic cell transplantation for thalassemia and sickle cell disease: past, present and future. *Bone Marrow Transplantation*. 2008;41(2):109-117. doi:10.1038/sj.bmt.1705943
73. Simon E, Long B, Koyfman A. Emergency Medicine Management of Sickle Cell Disease Complications: An Evidence-Based Update. *The Journal of Emergency Medicine*. 2016;51(4):370-381. doi:10.1016/j.jemermed.2016.05.042
74. Yawn BP, Buchanan GR, Afenyi-Annan AN, et al. Management of sickle cell disease: summary of the 2014 evidence-based report by expert panel members. *JAMA*. 2014;312(10):1033-1048. doi:10.1001/jama.2014.10517
75. Almuqamam M, Diaz – Frias J, Malik M, Mohamed AA, Sedrak A. Emergency management of SCD pain crises: Current practices and playing variables. *Pediatric Hematology Oncology Journal*. 2018;3(2):37-41. doi:10.1016/j.phoj.2018.06.002
76. Vander Borgh M, Wyns C. Fertility and infertility: Definition and epidemiology. *Clinical Biochemistry*. 2018;62:2-10. doi:10.1016/j.clinbiochem.2018.03.012
77. Hales CM. Prevalence of Obesity and Severe Obesity Among Adults: United States, 2017–2018. 2020;(360):8.

78. Wharton S, Lau DCW, Vallis M, et al. Obesity in adults: a clinical practice guideline. *CMAJ*. 2020;192(31):E875-E891. doi:10.1503/cmaj.191707
79. Law DCG, Macle hose RF, Longnecker MP. Obesity and Time to Pregnancy. *Hum Reprod*. 2007;22(2):414-420. doi:10.1093/humrep/del400
80. Pasquali R, Pelusi C, Genghini S, Cacciari M, Gambineri A. Obesity and reproductive disorders in women. *Human Reproduction Update*. 2003;9(4):359-372. doi:10.1093/humupd/dmg024
81. van der Steeg JW, Steures P, Eijkemans MJC, et al. Obesity affects spontaneous pregnancy chances in subfertile, ovulatory women. *Human Reproduction*. 2008;23(2):324-328. doi:10.1093/humrep/dem371
82. Metwally M, Ong KJ, Ledger WL, Li TC. Does high body mass index increase the risk of miscarriage after spontaneous and assisted conception? A meta-analysis of the evidence. *Fertility and Sterility*. 2008;90(3):714-726. doi:10.1016/j.fertnstert.2007.07.1290
83. Mukherjee G, Khasgir G, Basu S, Mahmud N. Practical Guide in Infertility. Published online April 19, 2018.
84. Vural F, Vural B, Çakıroğlu Y. The Role of Overweight and Obesity in In Vitro Fertilization Outcomes of Poor Ovarian Responders. *BioMed Research International*. 2015;2015:e781543. doi:10.1155/2015/781543
85. Maged AM, Fahmy RM, Rashwan H, et al. Effect of body mass index on the outcome of IVF cycles among patients with poor ovarian response. *International Journal of Gynecology & Obstetrics*. 2019;144(2):161-166. doi:10.1002/ijgo.12706

86. Goldsammler M, Merhi Z, Buyuk E. Role of hormonal and inflammatory alterations in obesity-related reproductive dysfunction at the level of the hypothalamic-pituitary-ovarian axis. *Reprod Biol Endocrinol*. 2018;16(1):45. doi:10.1186/s12958-018-0366-6
87. De Pergola G, Maldera S, Tartagni M, Pannacciulli N, Loverro G, Giorgino R. Inhibitory Effect of Obesity on Gonadotropin, Estradiol, and Inhibin B Levels in Fertile Women. *Obesity*. 2006;14(11):1954-1960. doi:10.1038/oby.2006.228
88. Caillon H, Fréour T, Bach-Ngohou K, et al. Effects of female increased body mass index on in vitro fertilization cycles outcome. *Obesity Research & Clinical Practice*. 2015;9(4):382-388. doi:10.1016/j.orcp.2015.02.009
89. Jain A, Polotsky AJ, Rochester D, et al. Pulsatile Luteinizing Hormone Amplitude and Progesterone Metabolite Excretion Are Reduced in Obese Women. *The Journal of Clinical Endocrinology & Metabolism*. 2007;92(7):2468-2473. doi:10.1210/jc.2006-2274
90. Ye J. Mechanisms of insulin resistance in obesity. *Front Med*. 2013;7(1):14-24. doi:10.1007/s11684-013-0262-6
91. Shanik MH, Xu Y, Škrha J, Dankner R, Zick Y, Roth J. Insulin Resistance and Hyperinsulinemia: Is hyperinsulinemia the cart or the horse? *Diabetes Care*. 2008;31(Supplement 2):S262-S268. doi:10.2337/dc08-s264
92. Templeman NM, Skovsø S, Page MM, Lim GE, Johnson JD. A causal role for hyperinsulinemia in obesity. *Journal of Endocrinology*. 2017;232(3):R173-R183. doi:10.1530/JOE-16-0449
93. Silvestris E, de Pergola G, Rosania R, Loverro G. Obesity as disruptor of the female fertility. *Reprod Biol Endocrinol*. 2018;16(1):22. doi:10.1186/s12958-018-0336-z

94. Tannous A, Bradford AP, Kuhn K, Fought A, Schauer I, Santoro N. A randomised trial examining inflammatory signaling in acutely induced hyperinsulinemia and hyperlipidemia in normal weight women-the reprometabolic syndrome. *PLoS One*. 2021;16(3):e0247638. doi:10.1371/journal.pone.0247638
95. Gervais A, Battista MC, Carranza-Mamane B, Lavoie HB, Baillargeon JP. Follicular Fluid Concentrations of Lipids and Their Metabolites Are Associated With Intraovarian Gonadotropin-Stimulated Androgen Production in Women Undergoing In Vitro Fertilization. *The Journal of Clinical Endocrinology & Metabolism*. 2015;100(5):1845-1854. doi:10.1210/jc.2014-3649
96. Batushansky A, Zacharia A, Shehadeh A, et al. A Shift in Glycerolipid Metabolism Defines the Follicular Fluid of IVF Patients with Unexplained Infertility. *Biomolecules*. 2020;10(8):1135. doi:10.3390/biom10081135
97. Wang S, Wang J, Jiang Y, Jiang W. Association between blood lipid level and embryo quality during in vitro fertilization. *Medicine (Baltimore)*. 2020;99(13):e19665. doi:10.1097/MD.00000000000019665
98. Khalil SF, Mohktar MS, Ibrahim F. The Theory and Fundamentals of Bioimpedance Analysis in Clinical Status Monitoring and Diagnosis of Diseases. *Sensors*. 2014;14(6):10895-10928. doi:10.3390/s140610895
99. Rani PR, Begum J. Screening and Diagnosis of Gestational Diabetes Mellitus, Where Do We Stand. *J Clin Diagn Res*. 2016;10(4):QE01-QE04. doi:10.7860/JCDR/2016/17588.7689

100. World Health Organization. Diagnostic Imaging and Laboratory Technology. *Use of Anticoagulants in Diagnostic Laboratory Investigations*. World Health Organization; 2002. Accessed November 30, 2021. <https://apps.who.int/iris/handle/10665/65957>
101. Matyash V, Liebisch G, Kurzchalia TV, Shevchenko A, Schwudke D. Lipid extraction by methyl-tert-butyl ether for high-throughput lipidomics ^[*]. *Journal of Lipid Research*. 2008;49(5):1137-1146. doi:10.1194/jlr.D700041-JLR200
102. Fiehn O. Metabolomics by Gas Chromatography–Mass Spectrometry: Combined Targeted and Untargeted Profiling. *Current Protocols in Molecular Biology*. 2016;114(1). doi:10.1002/0471142727.mb3004s114
103. Contaifer D, Buckley LF, Wohlford G, et al. Metabolic modulation predicts heart failure tests performance. *PLoS One*. 2019;14(6):e0218153. doi:10.1371/journal.pone.0218153
104. Hoaglin DC, Iglewicz B, Tukey JW. Performance of Some Resistant Rules for Outlier Labeling. *Journal of the American Statistical Association*. 1986;81(396):991-999. doi:10.1080/01621459.1986.10478363
105. van den Berg RA, Hoefsloot HC, Westerhuis JA, Smilde AK, van der Werf MJ. Centering, scaling, and transformations: improving the biological information content of metabolomics data. *BMC Genomics*. 2006;7(1):142. doi:10.1186/1471-2164-7-142
106. Burla B, Arita M, Arita M, et al. MS-based lipidomics of human blood plasma: a community-initiated position paper to develop accepted guidelines. *Journal of Lipid Research*. 2018;59(10):2001-2017. doi:10.1194/jlr.S087163
107. Antonelli J, Claggett BL, Henglin M, et al. Statistical Workflow for Feature Selection in Human Metabolomics Data. *Metabolites*. 2019;9(7):143. doi:10.3390/metabo9070143

108. Reddi AS. Acid-Base Disorders in Pregnancy. In: Reddi AS, ed. *Acid-Base Disorders: Clinical Evaluation and Management*. Springer International Publishing; 2020:299-303. doi:10.1007/978-3-030-28895-2_19
109. Song J, Xiang S, Pang C, Guo J, Sun Z. Metabolomic alternations of follicular fluid of obese women undergoing in-vitro fertilization treatment. *Sci Rep*. 2020;10(1):5968. doi:10.1038/s41598-020-62975-z
110. Oldham WM, Clish C, Yang Y, Loscalzo J. Hypoxia-mediated Increases in L-2-hydroxyglutarate Coordinate the Metabolic Response to Reductive Stress. *Cell Metab*. 2015;22(2):291-303. doi:10.1016/j.cmet.2015.06.021
111. Harris AL. A New Hydroxy Metabolite of 2-Oxoglutarate Regulates Metabolism in Hypoxia. *Cell Metabolism*. 2015;22(2):198-200. doi:10.1016/j.cmet.2015.07.016
112. Astudillo AM, Meana C, Bermúdez MA, Pérez-Encabo A, Balboa MA, Balsinde J. Release of Anti-Inflammatory Palmitoleic Acid and Its Positional Isomers by Mouse Peritoneal Macrophages. *Biomedicines*. 2020;8(11):480. doi:10.3390/biomedicines8110480
113. Sutton-McDowall ML, Gilchrist RB, Thompson JG. The pivotal role of glucose metabolism in determining oocyte developmental competence. *Reproduction*. 2010;139(4):685-695. doi:10.1530/REP-09-0345
114. Dunning KR, Russell DL, Robker RL. Lipids and oocyte developmental competence: the role of fatty acids and β -oxidation. *Reproduction*. 2014;148(1):R15-R27. doi:10.1530/REP-13-0251

115. Kindzelskii AL, Huang JB, Chaiworapongsa T, et al. Pregnancy alters glucose-6-phosphate dehydrogenase trafficking, cell metabolism, and oxidant release of maternal neutrophils. *J Clin Invest.* 2002;110(12):1801-1811. doi:10.1172/JCI15973
116. Lee J, Romero R, Dong Z, et al. Glycogen Phosphorylase Isoenzyme BB Plasma Concentration Is Elevated in Pregnancy and Preterm Preeclampsia. *Hypertension.* 2012;59(2):274-282. doi:10.1161/HYPERTENSIONAHA.111.177444
117. Sabbagh Y, Carpenter TO, Demay MB. Hypophosphatemia leads to rickets by impairing caspase-mediated apoptosis of hypertrophic chondrocytes. *Proc Natl Acad Sci U S A.* 2005;102(27):9637-9642. doi:10.1073/pnas.0502249102
118. Keskindepe L, Brackett BG. In Vitro Developmental Competence of in Vitro-Matured Bovine Oocytes Fertilized and Cultured in Completely Defined Media1. *Biology of Reproduction.* 1996;55(2):333-339. doi:10.1095/biolreprod55.2.333
119. Keskindepe L, Burnley CA, Brackett BG. Production of viable bovine blastocysts in defined in vitro conditions. *Biol Reprod.* 1995;52(6):1410-1417. doi:10.1095/biolreprod52.6.1410
120. Lynch CJ, Adams SH. Branched-chain amino acids in metabolic signalling and insulin resistance. *Nat Rev Endocrinol.* 2014;10(12):723-736. doi:10.1038/nrendo.2014.171
121. Tanianskii DA, Jarzebska N, Birkenfeld AL, O'Sullivan JF, Rodionov RN. Beta-Aminoisobutyric Acid as a Novel Regulator of Carbohydrate and Lipid Metabolism. *Nutrients.* 2019;11(3):524. doi:10.3390/nu11030524
122. Hemmings KE, Leese HJ, Picton HM. Amino Acid Turnover by Bovine Oocytes Provides an Index of Oocyte Developmental Competence In Vitro1. *Biology of Reproduction.* 2012;86(5). doi:10.1095/biolreprod.111.092585

123. Elango R, Ball RO. Protein and Amino Acid Requirements during Pregnancy. *Advances in Nutrition*. 2016;7(4):839S-844S. doi:10.3945/an.115.011817
124. Liu D, Mo G, Tao Y, et al. Putrescine supplementation during in vitro maturation of aged mouse oocytes improves the quality of blastocysts. *Reprod Fertil Dev*. 2017;29(7):1392-1400. doi:10.1071/RD16061
125. Lamb S, Aye CYL, Murphy E, Mackillop L. Multidisciplinary management of ornithine transcarbamylase (OTC) deficiency in pregnancy: essential to prevent hyperammonemic complications. *BMJ Case Rep*. 2013;2013:bcr2012007416. doi:10.1136/bcr-2012-007416
126. Malapaka RRV, Khoo S, Zhang J, et al. Identification and Mechanism of 10-Carbon Fatty Acid as Modulating Ligand of Peroxisome Proliferator-activated Receptors *. *Journal of Biological Chemistry*. 2012;287(1):183-195. doi:10.1074/jbc.M111.294785
127. Vanden Berghe W, Vermeulen L, Delerive P, De Bosscher K, Staels B, Haegeman G. A Paradigm for Gene Regulation: Inflammation, NF- κ B and PPAR. In: Roels F, Baes M, De Bie S, eds. *Peroxisomal Disorders and Regulation of Genes*. Advances in Experimental Medicine and Biology. Springer US; 2003:181-196. doi:10.1007/978-1-4419-9072-3_22
128. Valckx SD, Arias-Alvarez M, De Pauw I, et al. Fatty acid composition of the follicular fluid of normal weight, overweight and obese women undergoing assisted reproductive treatment: a descriptive cross-sectional study. *Reproductive Biology and Endocrinology*. 2014;12(1):13. doi:10.1186/1477-7827-12-13
129. Chen X, Stein TP, Steer RA, Scholl TO. Individual free fatty acids have unique associations with inflammatory biomarkers, insulin resistance and insulin secretion in healthy and gestational diabetic pregnant women. *BMJ Open Diabetes Res Care*. 2019;7(1):e000632. doi:10.1136/bmjdr-2018-000632

130. Wei Y, Wang D, Topczewski F, Pagliassotti MJ. Saturated fatty acids induce endoplasmic reticulum stress and apoptosis independently of ceramide in liver cells. *American Journal of Physiology-Endocrinology and Metabolism*. 2006;291(2):E275-E281.
doi:10.1152/ajpendo.00644.2005
131. Gomez E, Canela N, Herrero P, et al. Metabolites Secreted by Bovine Embryos In Vitro Predict Pregnancies That the Recipient Plasma Metabolome Cannot, and Vice Versa. *Metabolites*. 2021;11(3):162. doi:10.3390/metabo11030162
132. Marei WF, Wathes DC, Fouladi-Nashta AA. The Effect of Linolenic Acid on Bovine Oocyte Maturation and Development1. *Biology of Reproduction*. 2009;81(6):1064-1072.
doi:10.1095/biolreprod.109.076851
133. Ho CKM, Christenson LK, Strauss JF. CHAPTER 6 - Intracellular Cholesterol Dynamics in Steroidogenic Cells. In: Leung PCK, Adashi EY, eds. *The Ovary (Second Edition)*. Academic Press; 2004:93-110. doi:10.1016/B978-012444562-8/50007-0
134. Wathes DC, Abayasekara DRE, Aitken RJ. Polyunsaturated Fatty Acids in Male and Female Reproduction1. *Biology of Reproduction*. 2007;77(2):190-201.
doi:10.1095/biolreprod.107.060558
135. Dudzik D, Zorawski M, Skotnicki M, et al. Metabolic fingerprint of Gestational Diabetes Mellitus. *Journal of Proteomics*. 2014;103:57-71. doi:10.1016/j.jprot.2014.03.025
136. Knuplez E, Marsche G. An Updated Review of Pro- and Anti-Inflammatory Properties of Plasma Lysophosphatidylcholines in the Vascular System. *Int J Mol Sci*. 2020;21(12):4501.
doi:10.3390/ijms21124501

137. Heimerl S, Fischer M, Baessler A, et al. Alterations of Plasma Lysophosphatidylcholine Species in Obesity and Weight Loss. *PLOS ONE*. 2014;9(10):e111348.
doi:10.1371/journal.pone.0111348
138. Tan ST, Ramesh T, Toh XR, Nguyen LN. Emerging roles of lysophospholipids in health and disease. *Progress in Lipid Research*. 2020;80:101068.
doi:10.1016/j.plipres.2020.101068
139. Boots CE, Jungheim ES. Inflammation and Human Ovarian Follicular Dynamics. *Semin Reprod Med*. 2015;33(4):270-275. doi:10.1055/s-0035-1554928
140. Kumar NG, Contaifer D, Madurantakam P, et al. Dietary Bioactive Fatty Acids as Modulators of Immune Function: Implications on Human Health. *Nutrients*. 2019;11(12):2974. doi:10.3390/nu11122974
141. Ferchaud-Roucher V, Barner K, Jansson T, Powell TL. Maternal obesity results in decreased syncytiotrophoblast synthesis of palmitoleic acid, a fatty acid with anti-inflammatory and insulin-sensitizing properties. *FASEB J*. 2019;33(5):6643-6654.
doi:10.1096/fj.201802444R
142. Pietrantoni E, Del Chierico F, Rigon G, et al. Docosahexaenoic Acid Supplementation during Pregnancy: A Potential Tool to Prevent Membrane Rupture and Preterm Labor. *Int J Mol Sci*. 2014;15(5):8024-8036. doi:10.3390/ijms15058024
143. Petkevicius K, Virtue S, Bidault G, et al. Accelerated phosphatidylcholine turnover in macrophages promotes adipose tissue inflammation in obesity. Czech M, Rath S, eds. *eLife*. 2019;8:e47990. doi:10.7554/eLife.47990

144. de la Barca JMC, Boueilh T, Simard G, et al. Targeted metabolomics reveals reduced levels of polyunsaturated choline plasmalogens and a smaller dimethylarginine/arginine ratio in the follicular fluid of patients with a diminished ovarian reserve. *Human Reproduction*. 2017;32(11):2269-2278. doi:10.1093/humrep/dex303
145. Prates EG, Nunes JT, Pereira RM. A Role of Lipid Metabolism during Cumulus-Oocyte Complex Maturation: Impact of Lipid Modulators to Improve Embryo Production. *Mediators Inflamm*. 2014;2014:692067. doi:10.1155/2014/692067
146. Várnagy Á, Bene J, Sulyok E, Kovács GL, Bódis J, Melegh B. Acylcarnitine esters profiling of serum and follicular fluid in patients undergoing in vitro fertilization. *Reprod Biol Endocrinol*. 2013;11(1):67. doi:10.1186/1477-7827-11-67
147. Henrique C, Mansouri A, Fumey G, et al. Increased Mitochondrial Fatty Acid Oxidation Is Sufficient to Protect Skeletal Muscle Cells from Palmitate-induced Apoptosis. *J Biol Chem*. 2010;285(47):36818-36827. doi:10.1074/jbc.M110.170431
148. Aardema H, Vos PLAM, Lolicato F, et al. Oleic Acid Prevents Detrimental Effects of Saturated Fatty Acids on Bovine Oocyte Developmental Competence¹. *Biology of Reproduction*. 2011;85(1):62-69. doi:10.1095/biolreprod.110.088815
149. Conrad KP, Taher S, Chi YY, et al. Relationships between reproductive hormones and maternal pregnancy physiology in women conceiving with or without in vitro fertilization. *Am J Physiol Regul Integr Comp Physiol*. 2021;321(3):R454-R468. doi:10.1152/ajpregu.00174.2020
150. Bainbridge SA, Roberts JM. Uric Acid as a Pathogenic Factor in Preeclampsia. *Placenta*. 2008;29(Suppl A):S67-S72. doi:10.1016/j.placenta.2007.11.001

151. Shevell T, Malone FD, Vidaver J, et al. Assisted Reproductive Technology and Pregnancy Outcome. *Obstetrics & Gynecology*. 2005;106(5 Part 1):1039-1045.
doi:10.1097/01.AOG.0000183593.24583.7c
152. Gui J, Ling Z, Hou X, Fan Y, Xie K, Shen R. In vitro fertilization is associated with the onset and progression of preeclampsia. *Placenta*. 2020;89:50-57.
doi:10.1016/j.placenta.2019.09.011
153. Ruebel ML, Piccolo BD, Mercer KE, et al. Obesity leads to distinct metabolomic signatures in follicular fluid of women undergoing in vitro fertilization. *American Journal of Physiology-Endocrinology and Metabolism*. 2019;316(3):E383-E396. doi:10.1152/ajpendo.00401.2018
154. Savini I, Catani MV, Evangelista D, Gasperi V, Avigliano L. Obesity-Associated Oxidative Stress: Strategies Finalized to Improve Redox State. *International Journal of Molecular Sciences*. 2013;14(5):10497-10538. doi:10.3390/ijms140510497
155. Zhou Y, Qiu L, Xiao Q, et al. Obesity and diabetes related plasma amino acid alterations. *Clinical Biochemistry*. 2013;46(15):1447-1452. doi:10.1016/j.clinbiochem.2013.05.045
156. Wang N, Wei J, Liu Y, et al. Discovery of biomarkers for oxidative stress based on cellular metabolomics. *Biomarkers*. 2016;21(5):449-457. doi:10.3109/1354750X.2016.1153720
157. Kalhan SC, Gilfillan CA, Tserng KY, Savin SM. Glucose-alanine relationship in normal human pregnancy. *Metabolism*. 1988;37(2):152-158. doi:10.1016/S0026-0495(98)90010-5
158. Zhang C mei, Zhao Y, Li R, et al. Metabolic heterogeneity of follicular amino acids in polycystic ovary syndrome is affected by obesity and related to pregnancy outcome. *BMC Pregnancy and Childbirth*. 2014;14(1):11. doi:10.1186/1471-2393-14-11

159. D'Aniello G, Grieco N, Di Filippo MA, et al. Reproductive implication of d -aspartic acid in human pre-ovulatory follicular fluid. *Human Reproduction*. 2007;22(12):3178-3183.
doi:10.1093/humrep/dem328
160. Topo E, Soricelli A, D'Aniello A, Ronsini S, D'Aniello G. The role and molecular mechanism of D-aspartic acid in the release and synthesis of LH and testosterone in humans and rats. *Reproductive Biology and Endocrinology*. 2009;7(1):120. doi:10.1186/1477-7827-7-120
161. Casarini L, Santi D, Brigante G, Simoni M. Two Hormones for One Receptor: Evolution, Biochemistry, Actions, and Pathophysiology of LH and hCG. *Endocrine Reviews*. 2018;39(5):549-592. doi:10.1210/er.2018-00065
162. Zhao Y, Fu L, Li R, et al. Metabolic profiles characterizing different phenotypes of polycystic ovary syndrome: plasma metabolomics analysis. *BMC Medicine*. 2012;10(1):153. doi:10.1186/1741-7015-10-153
163. Ma Q, Zhou X, Sun Y, et al. Threonine, but Not Lysine and Methionine, Reduces Fat Accumulation by Regulating Lipid Metabolism in Obese Mice. *J Agric Food Chem*. 2020;68(17):4876-4883. doi:10.1021/acs.jafc.0c01023
164. Vangipurapu J, Stancáková A, Smith U, Kuusisto J, Laakso M. Nine Amino Acids Are Associated With Decreased Insulin Secretion and Elevated Glucose Levels in a 7.4-Year Follow-up Study of 5,181 Finnish Men. *Diabetes*. 2019;68(6):1353-1358.
doi:10.2337/db18-1076
165. Rampler E, Abiead YE, Schoeny H, et al. Recurrent Topics in Mass Spectrometry-Based Metabolomics and Lipidomics—Standardization, Coverage, and Throughput. *Anal Chem*. 2021;93(1):519-545. doi:10.1021/acs.analchem.0c04698

Supplementary appendix:

1. Plasma data:

a. BMI

Variable selected	Prob> t	Model R ² and R ² adj
BMI and lipids with glycerophospholipids		
LPC (18:1)	0.0133	R ² = 0.839 R ² adj= 0.785 Root mean square error=0.138
LPC(22:6)	0.0127	
LPC (p-16:0)	0.0021	
PC(16:0-22:4)	0.0027	
PC(16:1-22:6)	0.0002	
PI(18:0-20:4)	0.0422	
BMI and lipids without glycerophospholipids		
CE (18:0)	0.0014	R ² = 0.794 R ² adj= 0.726 Root mean square error= 0.156
CE (20:3)	0.0015	
CE (22:4)	<.0001	
FA (14:1)	<.0001	
FA (17:1)	0.0005	

Heptadecanoic acid	0.0089	
BMI and metabolite model		
2-hydroxyglutaric acid	0.0189	$R^2 = 0.804$ $R^2 \text{ adj} = 0.739$ Root mean square error= 0.152
alanine	0.0144	
glucose-1-phosphate	0.0015	
Malic acid	0.0349	
serine	<.0001	
tyrosine	0.0157	
BMI and clinical parameter model		
Fasting glucose	0.3374	$R^2 = 0.807$ $R^2 \text{ adj} = 0.768$
Fasting Insulin	<.0001	
Total score Block food Fat screener 23 high	0.0054	
Average Sitting Total Minutes/day	0.1554	
Final plasma BMI model		
LPC (18:1)	0.0244	$R^2 = 0.856$ $R^2 \text{ adj} = 0.818$
PC (16:0-22:4)	0.0044	
PC (16:1-22:6)	0.0594	

Malic acid	0.0239	
Fasting insulin	0.0018	

b. 2PN

Variable selected	Prob> t	Model R ² and R ² adj
2PN and Lipids with glycerophospholipids		
LPC(22:6)	0.0213	R ² = 0.805 R ² adj= 0.730
LPE(20:4)	0.0005	
PC(14:0-16:1)	0.0060	
PC(16:1-22:6)	0.2452	
PE(18:0-20:3)	0.2569	
PE-P(16:0-20:5)	0.0013	
PE-P (16:0-22:6)	0.0004	
2PN and Lipids without glycerophospholipids		
CE(22:6)	0.00066	R ² = 0.799 R ² adj= 0.666
Lauric acid	0.01373	
CE (20:5)	0.02362	

FA(19:1)	0.02885	
CE(16:0)	0.06641	
Myristic acid	0.06739	
CE(14:0)	0.11267	
FA (20:5)	0.14690	
FA (18:2)	0.38866	
FA (14:1)	0.59931	
2PN and metabolite model		
2-ketoisovaleric acid	0.0001	R ² = 0.829 R ² adj= 0.749
3-aminoisobutyric acid	0.0004	
Aspartic acid	0.0236	
Beta alanine	0.0007	
Glutamic acid	0.0002	
ornithine	0.0225	
phosphate	0.0030	
serine	0.0033	
2PN and clinical parameter model		
Female age (yr)	0.4979	R ² = 0.623

Fasting glucose	0.1282	R ² adj= 0.445
Fasting insulin	0.9776	
Mediterranean diet score	0.1929	
Total score Block food Fat screener 23 high.	0.8744	
Total score Block food questionnaire fruit vegetable screener 11 low.	0.0712	
Average Sitting Total Minutes day	0.0221	
Total cumulative FSH used	0.0015	
Final plasma 2PN model tested for clinical parameter (Exclude the clinical parameter)		
LPC (22:6)	0.0057	R ² = 0.792
LPE (20:4)	0.0023	R ² adj= 0.726
PC(14:0-16:1)	0.0329	
CE (16:0)	0.0056	
FA (20:5)	0.0212	
phosphate	0.0003	

2. Follicular fluid:

a. BMI

Variable selected	Prob> t	Model R ² and R ² adj
-------------------	----------	---

BMI and with glycerophospholipids		
LPC(18:2)	0.0061	R ² = 0.839 R ² adj= 0.797
LPC (20:2.)	0.0280	
LPC(o-18:1)	0.0006	
PC (20:3-20:4)	0.0003	
PE-P(16:0-22:6)	<.0001	
BMI and without glycerophospholipids		
CE (16:0)	0.0236	R ² = 0.779 R ² adj= 0.705
CE (18:3)	0.0004	
CE(20:3)	<.0001	
FA (18:1)	0.0009	
FA(19:0)	0.0028	
FA(22:2)	0.0239	
BMI and metabolite model		
Aspartic acid	0.0003	R ² = 0.795 R ² adj= 0.754
histidine	0.0285	
Indole-3-propionic acid	0.0008	
tyrosine	<.0001	

Final BMI model		
PE-P(16:0-22:6)	0.0040	R ² = 0.880 R ² adj= 0.856
Aspartic acid	0.0141	
Indole-3-propionic acid	<.0001	
Fasting insulin	<.0001	

b. 2PN:

Variable selected	Prob> t 	Model R² and R² adj
2PN and with glycerophospholipids		
Acylcarnitine (C16:0)	0.0033	R ² = 0.833 R ² adj= 0.755
Acylcarnitine C18:1	0.0358	
LPC (16:1)	0.0047	
LPC (22:4)	0.0028	
LPE (20:4)	0.0042	
LPI (18:1)	0.0048	
LPI (18:2)	0.0023	
PC-P(18:0-22:6)	0.0013	
2PN and without glycerophospholipids		

CE (16:1)	0.0517	R ² = 0.813 R ² adj= 0.725
CE (18:1)	0.0009	
CE (18:3)	0.0732	
CE (22:6)	0.0003	
FA (14:0)	0.0410	
FA (16:0)	0.0404	
2PN and metabolite model		
1-monoolein	0.0834	R ² = 0.794 R ² adj= 0.729
2-aminobutyric acid	0.0021	
alanine	0.0003	
hexose	0.0010	
phenylalanine	0.0108	
phenylethylamine	0.0002	
Final 2PN model tested for clinical parameter		
LPE (20:4)	0.0040	R ² = 0.808 R ² adj= 0.747
PC-P(18:0-22:6)	0.0115	
2-aminobutyric acid	0.0934	
alanine	0.0062	

phenylethylamine	0.0564	
FA (22:3)	0.0438	